6-2007

CFD Investigation of Effect of Depth to Diameter Ratio on Dimple Flow // Computational fluid dynamics investigation of effect of depth to diameter ratio on dimple flow dynamics

Robert B. Etter

CFD Investigation of Effect of
Depth to Diameter Ratio on Dimple Flow Dynamics

THESIS

Robert B. Etter, Ensign, USN

AFIT/GAE/ENY/07-J07

DEPARTMENT OF THE AIR FORCE
AIR UNIVERSITY

AIR FORCE INSTITUTE OF TECHNOLOGY

Wright-Patterson Air Force Base, Ohio

APPROVED FOR PUBLIC RELEASE; DISTRIBUTION UNLIMITED

AFIT/GAE/ENY/07-J07

CFD Investigation of Effect of Depth to Diameter Ratio on Dimple Flow Dynamics

THESIS

Presented to the Faculty

Department of Aeronautics and Astronautics

Graduate School of Engineering and Management

Air Force Institute of Technology

Air University

Air Education and Training Command

In Partial Fulfillment of the Requirements for the

Degree of Master of Science in Aeronautical Engineering

Robert B. Etter, B.S.

Ensign, USN

June 2007

AFIT/GAE/ENY/07-J07

CFD Investigation of Effect of
Depth to Diameter Ratio on Dimple Flow Dynamics

Robert B. Etter, B.S.

Ensign, USN

Approved:

Lt Col Raymond C. Maple, PhD (Chairman)		date
Dr. Paul King (Member)		date
Dr. Mark F. Reeder (Member)		date

AFIT/GAE/ENY/07-J07

Abstract

This study aimed to further the understanding of laminar flow through a dimple with the goal of mitigating flow separation. Dimples of various depth to diameter ratios (0.05, 0.15) were examined for three different dimple diameters and chordwise locations, corresponding to diameter based (Re_D) and chordwise location based (Re_x) Reynolds number combinations of Re_D20500 Re_x5000, Re_D20500 Re_x77000, and Re_D9000 Re_x21000. For the last combination, a dimple of depth to diameter ratio of 0.25 was also examined. The dimples were placed in a flat plate located in a diverging channel causing an adverse pressure gradient encouraging flow separation near the dimple location. The flow was modeled in the commercial CFD solver Fluent. Results indicate that dimple depth to diameter ratio has a significant effect on the structure of dimple flow. The shallowest dimples showed little change to the overall flow in the channel. Deeper dimples contained dynamic vortical flow structures with behavior varying between each dimple studied. This dynamic vortex activity was observed to be linked with variances in downstream flow. The 0.15 depth to diameter ratio dimples showed behavior very similar to 0.10 ratio dimples investigated elsewhere. The 0.25 dimple show flow different in nature than 0.15 dimples for the same Re_D and Re_x; the differences were not as stark as those between 0.05 and 0.15 dimples. In light of this and other studies, dimple flow behavior is found to depend on a combination of parameters that eludes direct quantitative parameterization. However, the conclusion is drawn that the most effective dimple will be just deep enough to develop dynamic vortical activity and vortex shedding.

Acknowledgements

I would like to thank 1Lt Robert Vincent for assisting me in the building and setup of my grids and Fluent jobs. I would also like to thank Capt. Matt Caspers for his continual advice and assistance in Fluent, Ensight, VTK, and Linux.

Robert B. Etter

Table of Contents

List of Figures

List of Tables

Nomenclature

Symbol	Description
ν	Kinematic viscosity (m^2/s)
D	Dimple diameter
x	chordwise location
Re	Reynolds number
Re_D	Diameter based Reynolds number $\nu * v * D$
Re_x	Chord based Reynolds number $\nu * v * x$

Abbreviations

Abbreviation	Description
CFD	Computational Fluid Dynamics
FVE	Fluent VTK Extractor
VTK	Visualization Toolkit
PSD	Power Spectrum Density
h/D	Dimple Depth to Diameter Ratio

CFD Investigation of Effect of
Depth to Diameter Ratio on Dimple Flow Dynamics

I. Introduction

High altitude reconnaissance can provide valuable military intelligence over a wide area. If an aircraft is able to loiter over a particular area, it can provide near real-time information. Unmanned Air Vehicles (UAVs) have become popular choices for this mission due to their range and endurance. However, UAVs operating in this role are being limited by inefficiencies in the low pressure turbines (LPT) of their powerplants. The combination of the high altitude and low speed flight envelope desired for high altitude reconnaissance results in low Reynolds numbers and, subsequently, laminar flow in the LPT. Inefficiencies arise as the flow separates over the LPT blades. Shallow dimples have shown promise in limiting separation, and are very attractive due to their passivity and the ease of implementation into existing blades.

1.1 Research Goals

The exact nature of the flow in and downstream of the dimple is not fully understood. Questions remain as to how different parameters, such as depth, diameter, and placement affect the flow dynamics in the dimple. This research aims to examine the effects that dimple depth to diameter ratio has on dimple flow dynamics in laminar flow subject to an adverse pressure gradient sufficient to cause flow separation

1.2 Motivation for Research

Flow separation in the low pressure turbine results in significant efficiency losses in the gas turbine. Separated flow causes a drop in total pressure through the engine. Lake [6] showed that the engine efficiency could be increased by 0.057% for every percent reduction in total pressure loss. An increase in engine efficiency translates

directly into an increase in range, or a corresponding increase in payload or decrease in fuel consumption. Mechanisms to control boundary layer separation may initially be divided into two types: active and passive. Active boundary layer control, such as suction and blowing, can offer more effective boundary layer control. However, it is much more complex to implement, increasing both weight and cost of an engine. Also, it is much harder to implement after engine construction.

Passive flow control generates greater interest because of its low cost, both in installation and maintenance. Passive techniques typically rely on generating vortices to energize flow in order to overcome adverse pressure gradients. Protruding passive flow control devices produce streamwise vortices. These vortices are generally quite stable and are able to energize the flow far downfield. Recessed passive flow control may consist of dimples, grooves, or porus cavities. While they do not mix downstream flow as effectively as protruding devices, they offer a smaller drag penalty when used outside their design envelope.

James Lake [6] performed an examination of passive techniques in suppressing boundary layer separation on a Pak-B turbine blade. He examined the effectiveness of dimpels, v-grooves, and trip wires in reducing losses due to separation. He placed a row of elliptical dimples (with major axis perpendicular to the flow direction) at several different axial chord locations. Lake found that the dimples offered significant improvement over the baseline Pak-B blade in mitigating separation losses. He was able to consistently reduce total pressure loss coefficient by more than 40% when using dimples.

At a Reynolds number of 50k and low freestream turbulence, the unmodified Pak-B blade had a large separation bubble. The bubble began at about 73% of the chord and reached a maximum above the blade at 89% of the chord. In the best dimple case, the separation bubble was much smaller. It had a maximum height about one sixth that of the separation bubble on the unmodified blade. Turbulence profiles reveal greater turbulence for the dimpled case near the surface of the blade,

but less throughout the boundary layer/separated region. The turbulence intensity profiles of the dimpled case reflected those of unseparated flow. Lake compared the use of dimples to trip wires and v-grooves; dimples proved superior to both.

1.3 Research Approach

Dimples of varying depths will be analyzed with the commercial Computational Fluid Dynamics (CFD) code Fluent. The dimples will be located on a flat plate. An infinite span of dimples will be simulated. To simulate the condition of separation on a turbine blade, an adverse pressure gradient will be implemented. This investigation aims to further the understanding of flow characteristics within the dimple. To this end, exact replication of quantities such as vortex shedding frequencies, pressure variations and magnitude and velocity profiles from Pak-B turbine blades is unnecessary. Essentially, this investigation studies the flow behavior in dimples of various depth to diameter ratios on a flat plate in an adverse pressure gradient enforced by a diverging top wall.

1.4 Outline of Thesis

Chapter one presents an introduction to the investigation and motivation for the study. Chapter two gives background on dimple flow leading to this study. Chapter three describes the methodology used in this research, including a description of the software used. Chapter four present the results of the investigation and analysis. Chapter five summarizes the study and provides suggestions for future study.

II. Background and Theory

Research has been done on dimples for a broad range of applications and flow regimes. However, many of these applications involve turbulent flow. Research on laminar flow in dimples is much harder to come by. Some investigations have been made that may provide information applicable to optimizing dimple usage for mitigating separation on low pressure turbine blades.

2.1 Previous Research on Dimples

In order to determine what characteristics of dimples still need to be studied, an overview has been made of previous investigations. Earlier research has already determined the effect and optimum usage of several different dimple characteristics and parameters.

James Lake [6] examined dimple location along with comparing dimples to v-grooves and trip wires in his investigation on reducing sparation on a Pak-B turbine blades. He found that dimple location had an effect on dimple effectiveness. Dimples were most effective when placed slightly upstream of the unmodified blade separation point. As the dimple was moved further upstream of the separation point, its effectiveness decreased. His research shows that for maximum effect, dimples should be placed as closely as possible to the point of separation.

Kurt Rouser [10] expanded on the research of James Lake. He tested different dimple shapes, an elliptical dimple and a half ellipse symmetrical dimple cut in the direction of the flow. Both of these dimple shapes were compared to the baseline Pak-B blade. Rouser's results from both experimental and CFD investigation revealed that the larger, symmetric dimple was more effective in controling separation and increasing efficiency of the turbine blade.

John Casey [2] continued the investigation of dimples as a method of boundary layer control on a Pak-B low pressure turbine blade. He tested different patterns and spanwise spacing of dimples with both a wind tunnel and CFD. Casey found that increasing the spacing between dimples in a single row did not substantially

affect separation performance. He also investigated adding a second row of dimples staggered from the first. Casey observed that while this configuration did alter the flow dynamics, it did not offer better performance. He concluded that a single row of dimples with spacing near one dimple diameter was the best configuration.

Robert Vincent [14] carried out a detailed CFD examination of flow dynamics within a spherical dimple. In an effort to separate boundary layer effects from dimple diameter effects, Vincent investigated a number of different flow geometries. He varied two parameters, Re_x (by changing streamwise dimple location) and Re_D (by changing dimple diameter). He held dimple depth to diameter ratio to a constant 0.1. Vincent found that changing Re_D and Re_x had significant impact on dimple flow dynamics. He observed that stronger (more stable) vortices existed in dimples with high boundary layer momentum compared to dimple diameter (i.e., high Re_x and low Re_D) to a point. Flow through the dimple became much more disorganized if Re_D increased and Re_x decreased beyond a certain range.

The research of Lake and Casey has done much to help optimize the location and layout of dimples on a turbine blade. Rouser's work provided information on how dimple flow may be influenced by changing shape. Vincent's investigation provided information on the effect of changing dimple geometry. It also shed light on the flow dynamics through the dimple, and how changes in geometry affect the flow. However, Vincent isolated only one dimple geometry parameter. Changing other dimple geometry parameters may have an impact on dimple flow dynamics and need to be investigated in order to determine optimal dimple shape.

2.2 Dimple Flow Dynamics

Having established dimple parameters that have already been studied, the next step is to determine what parameter most warrants further investigation. To do this, it is important to understand the nature of the flow through a dimple. How and why the dimple affects downstream flow is also important. Using previous research

to develop an understanding of these factors will lead to a better prediction of which dimple characteristic would be most benefical to study further.

2.2.1   Flow Through a Dimple.   Rouser found a vortex core stretched across both the symmetric and asymmetric dimples. He suggested that the trapped vortex within the dimple and the flow it entrained were the strongest contributors to the increase in efficiency observed by Lake. Furthermore, Rouser concluded from his CFD investigation that the flow through the dimple was fundamentally unsteady. Casey also found a vortex contained within the dimple defined by a separation line on the dimple leading edge and a reattachment line on the dimple trailing edge. This suggests the vortex found by Rouser occupies most of the dimple. Casey also found that the flow was drawn towards the center of the dimple before being expelled, shedding some light on the vortex orientation within the dimple.

Ligrani [7] offers a qualitative description of flow through a dimple. Smoke lines revealed that flow was drawn from above the dimple to impact on the downstream rim. Accompanying this were pairs of recirculation zones within the dimple. Then, flow from the central part of the dimple moved upward and was ejected. As flow was ejected from the dimple center, flow moved in from the dimple sides to take its place. The ejected flow formed a pair of steamwise counter-rotating vortices. This vortex pair was stretched downstream, and new flow was drawn into the dimple. Figure 2.1 provides futher detail.

Ligrani's description of dimple flow suggests that changing dimple depth may have impact on dimple flow. A deeper dimple with respect to dimple diameter may draw flow in more severely (greater change in streamline direction). Also, when the flow is expelled from the dimple, the greater amount of flow to be expelled combined with the smaller cross sectional area through which the flow is expelled may result in stronger vortices emerging from the dimple.

However, analogies from cavity flow suggest changing dimple depth may fundamentally alter flow dynamics. In general, cavities may be thought of as open or closed

t (sec.)

.000

.017

.033

.050

.067

.083
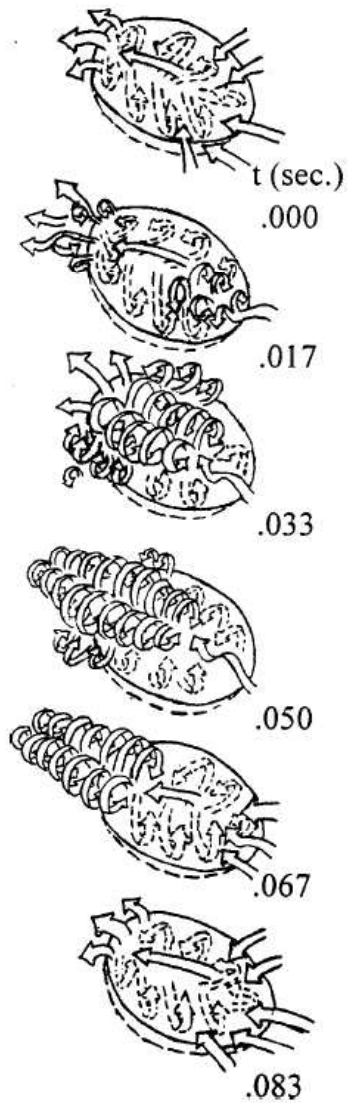
Figure 2.1:   Ligrani's suggestion of the cycle of flow through a dimple [7]

7

with a depth to length ratio of 1/8 dividing the two rectangular cavities [5]. In open cavities, flow separates at the leading edge and reattaches at the cavity trailing edge. In a closed cavity, flow reattaches on the cavity bottom before reaching the trailing edge. Grace [5] and Ozsoy [9] examined laminar flow in a rectangular cavity with a depth to length ratio of 0.25 and found two spanwise counter rotating vortices fully contained within the cavity. The only significant downstream flow effect was an increase in boundary layer thickness. While any cutoff between open and closed flow in dimples may be different than in rectangular cavities, the same principle (significant change in flow dynamics with a change in depth) still may apply.

Vincent [14] investigated dimples with a number of different diameter and chord based Reynolds numbers. Unlike Casey and Rouser, he focused his research on the flow dynamics within the dimple itself. Unlike Ligrani, he used a CFD approach, allowing him to get much better detail on the flow within the dimple. Vincent noticed a number of flow characteristics common to most of the dimples that corroborated Casey and Rouser. A separation line was located at the dimple leading edge and a reattachment line at the trailing edge. Vincent was able to further resolve the nature of the vortex flow within the dimple. He observed a wake zone towards the stern of the dimple characterized by large, disorganized vortical activity and vortex shedding. A recirculation zone in the bow of the dimple was dominated by pinned vortices. The typical location and makeup of these zones is shown in Figure 2.2.

Vincent was able to divide his results into three principles classes depending upon the character of the dimple flow. One class of dimples was characterized by contained, highly chaotic wake structures. This class also contained a much larger and more chaotic wake region. Another class was characterized by more organized vortices periodically forming and shedding. The third class showed little wake and little effect on the flow. In this case, the wake region has disappeared leaving symmetric flow. A larger Re_D (larger dimple diameter) encouraged greater flow mixing and a more chaotic structure, while a larger Re_x (thicker boundary layer) seemed to reduce the effect of the dimple on the flow. Vincent suggested that the amount of energy entering
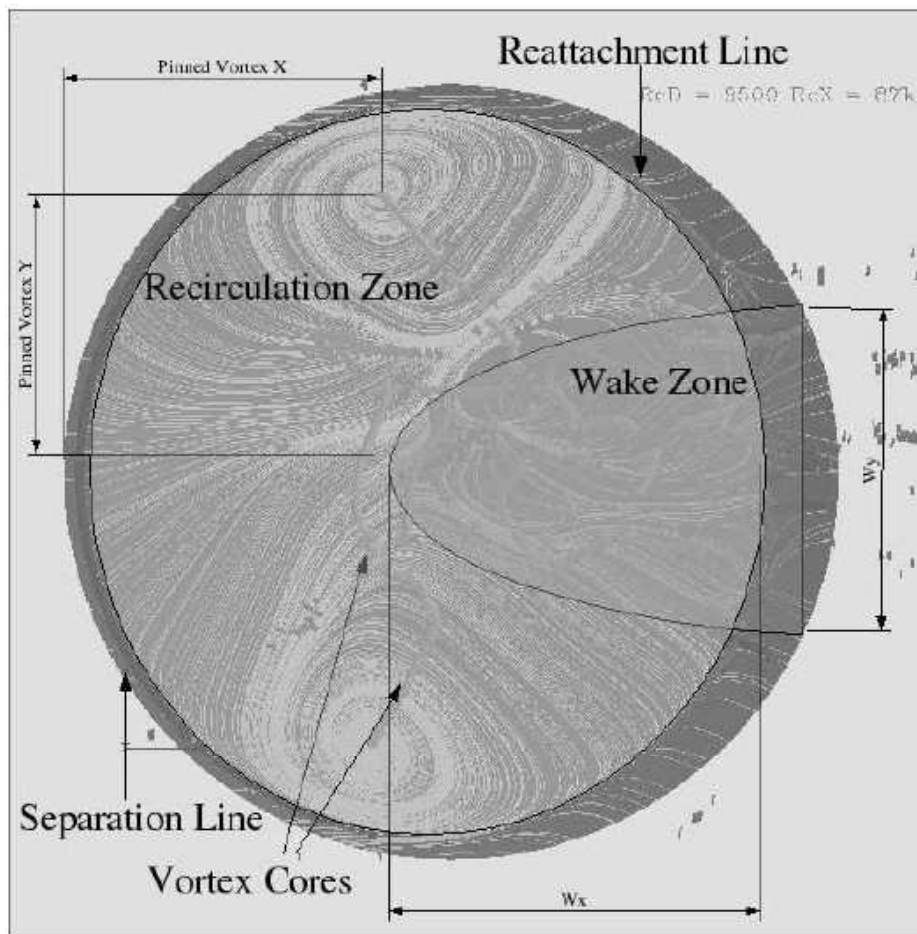
Figure 2.2: Vincent's breakdown of the wake and recirculation zones observed within the dimple and identification of typical vortex cores [14]

the dimple could be an important parameter in determining the nature of the flow within. He qualitatively characterized energy by boundary layer thickness and dimple diameter; a thicker boundary layer introduces less energy into the dimple, and a larger diameter more energy. Vincent also suggested that the character of the vortices within the dimple depended upon Re_D and Re_x. He observed that stronger (more stable) vortices existed in dimples with high boundary layer momentum compared to dimple diameter. These results reveal that altering dimple diameter may have a significant affect on flow dynamics. However, Vincent maintained a constant dimple depth to diameter ratio. Because of this, effects observed when changing Re_D (i.e. dimple diameter) may have been due rather to changing dimple depth.

2.2.2   Flow Effects Downstream.   The purpose of using dimples is to alter downstream flow. To this end, it is important to understand how and why dimples change the flow downstream. This will provide an indication of what flow dynamics in a dimple are favorable for mitigating flow separation. Rouser [10] concluded that vortices caused by the dimple entrained flow, leading to better separation performance. Casey [2] observed cycles of reattachment and separation downstream of the dimple. This suggested that the shedding of vortices from the dimple played a roll in combating flow separation.

Ligrani [7] made an interesting observation connecting vorticity magnitudes and flow mixing. He found that time averaged streamwise vorticity and maximum normalized Reynolds normal stress $((\overline{u'^2}/\overline{U^2})_{max})$ followed similar trends. Furthermore, Ligrani found that the locations of vortex pairs near the dimpled surface corresponded well with locations where normalized Reynolds normal stress was increased. Flow mixing seems to be a primary method by which separation is reduced [14], and Ligrani [7] showed that vorticity has a direct effect on flow mixing. Hence higher streamwise vorticity generation is a desirable dimple trait.

Vincent [14] observed pressure waves in his CFD analysis resulting from impact of shedding vortices upon the trailing edge of the dimple. These pressure waves had

a frequency of order 100 Hz, with frequency increasing with Re_D. Vincent concluded that the largest benefits of the dimple could be obtained with high speed shedding. The shedding of vortices served to mix the flow and alleviate separation. He found that shedding frequency had a strong dependence on dimple size; large dimples (high Re_D) had fairly constant frequencies while medium dimples had variable shedding frequencies. Small diameter dimples showed no shedding. The higher Re_D and lower Re_x cases also displayed an occasional shedding of the entire vortex within the dimple. Dimples between small and large diameter showed vortex shedding alternating side to side across the dimple, similar to Von Karman shedding. Again, however, because Vincent linked diameter and depth, the changes he noticed from increasing diameter may have been due to increasing dimple depth.

2.3 Use of CFD

Several previous studies have verified the applicability of CFD to studying dimple flow dynamics. Rouser [10] found that the total pressure loss coefficient computed from CFD and wind tunnel experiments closely matched each other. Casey found that CFD boundary layer profiles were qualitatively similar to experimental data. The boundary layer profiles and the total pressure loss coefficients followed similar trends. This suggests that CFD may be used to qualitatively investigate dimple flow dynamics.

However, Rouser found that turbulence models he used were unable to capture separation on the Pak-B turbine blade. He tested Spalart-Allamras, K-ω, and K-ε models. Hence, he (along with Casey [2] and Vincent [14]) used laminar models. While laminar solvers proved able to simulate flow inside of the dimple, downstream of the dimple Casey found that experimental and CFD data began to differ substantially. This is likely the result of much more complex, turbulent flow downstream of the dimple. Because of this, data taken from a laminar CFD solver from far downstream of the dimple should be examined with great caution.

2.4 Implications for this Research

Previous research has already established the effect of some parameters in using dimples to reduce losses due to laminar flow separation on a Pak-B turbine blade. Dimple location on the blade, basic dimple geometry, and dimple spacing patterns have already been investigated. So too have more precise dimple geometric characteristics such as dimple diameter. However, this leaves several dimple characteristics left to study. A study of known qualities of flow through dimples reveals that dimple depth may be an interesting parameter to study. Changing dimple depth may alter flow characteristics. Vortex strength and shedding frequency may be affected by changing dimple depth, and this, in turn may change dimple effectiveness in mitigating flow separation.

III. Methodology

Computational Fluid Dynamics is a very complex process. Each stage, grid generation, flow solving, and visualization, must be understood in order to be used properly. Each step must not be viewed as a "black box". The strengths and weaknesses of different methods and software must be understood along with their application to the specific problem to be investigated.

3.1 Basic Geometry

A low pressure turbine has very complex geometry. A large number of blades are arranged to project radially, and each blade itself can have a complex geometry. Simplifications are necessary to reduce computing time and cost. Casey's investigation used an extrusion of a 2-D airfoil to model a cascade of turbine blades. Vincent's study went much further in the simplification.

Skyred [13] performed an investigation comparing flow dynamics of dimples on concave, convex, and flat surfaces. Although the Reynolds numbers used in his study were higher than the ones used here, the dimples displayed behavior similar to Vincents. Skyred found a similar flow pattern in all three geometries. The flow structure in the dimples seemed to be more self-organized than dependant upon dimple surface geometry. From Skyred's study, pressure gradient is seen to be a more important factor in dimple flow than domain shape.

As a consequence of Syreds study, Vincent determined that the complex geometry of a turbine blade could be replaced with a far simpler flat channel with an adverse pressure gradient sufficient for separation. The basic geometry used in this investigation is the same as that used by Vincent. As seen in Figure 3.1, the side walls are flat, as is the bottom wall with the exception of the dimple. Vincent enforced an adverse gradient by using a diverging top wall. Lake's [6] research found that dimples were most effective when placed near the point of flow separation on an unmodified airfoil. Hence, the dimple will be placed near the point of flow separation.
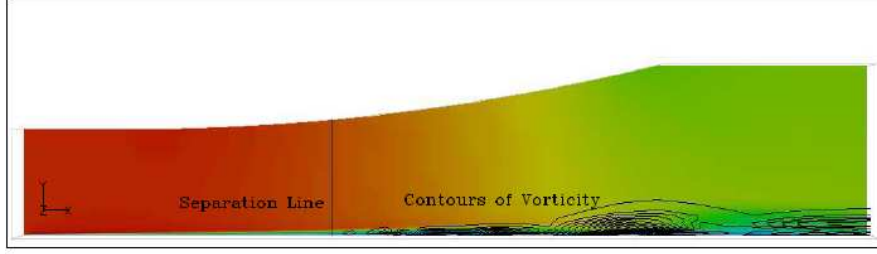
Figure 3.1:   Profile of channel created by Vincent [14], with sparation line identified

Vincent [14] determined the top wall geometry through trial and error on a flat plat channel. The following equation describes a top wall geometry that produces an adverse pressure gradient sufficient to cause separation near the middle of the channel without drawing vortices too far from the bottom wall. Separation is identified by reversed flow and a line of zero shear stress.

$$Z(x) = \begin{cases} 0.04995 + 0.0160601 * x + 0.376516x^2 + 0.371514 * x^3 & : & -0.06 \leq x \leq 0.2 \\ 0.15 & : & 0.2 < x \leq 0.34 \end{cases}$$

$$(3.1)$$

The role of the top wall is to enforce the adverse pressure gradient. It is not necessary to model a boundary layer on the top wall, so to reduce computational time and cost, it will be made an inviscid wall.

In order to simulate an infinite span of dimples, the side boundaries will be periodic. Casey found that spanwise dimple spacing did not significantly affect flow characteristics, thus dimple spacing is not a great issue. For convenience, Vincent's dimple spacing of 2 dimple diameters will be used. The channel itself will be 3 dimple diameters wide.

3.2   Flow Geometry

Three Re_x and Re_D combinations from Vincent's study will be used. One is a mid range case, with an Re_D of 9500 and Re_x of 21000. This case will be studied to see if changing dimple depth results in the character of the flow becoming more like

14

Table 3.1:   Geometric Paramaters of Each Dimple

Depth (m)	Diameter (M)	Depth to Diameter Ratio	x_{le} (m)	Re_D	Re_x
0.00065	0.013	0.05	0.0236	9500	21000
0.00195	0.013	0.15	0.0236	9500	21000
0.00325	0.013	0.25	0.0236	9500	21000
0.0015	0.03	0.05	0.0058	20500	5000
0.0045	0.03	0.15	0.0058	20500	5000
0.0014	0.03	0.05	0.1124	20500	77000
0.0045	0.03	0.15	0.1124	20500	77000

a case of higher or lower Re_D or Re_x. The other two values chosen reflect extremums of Vincents study; both have a high Re_D of 20500. One has a Re_x of 5000, the other 77000. These extreme cases may be more sensitive to the variation of dimple depth. For each case, a dimple depth to diameter ratio of 0.05 and 0.15 will be tested (a 50% increase and decrease from Vincents ratio of 0.10). Additionally, a depth to diameter ratio of 0.25 will be tested on the mid range case. The higher dimple depths may result in fundamental changes to dimple flow dynamics, as suggested by study of laminar flow in shallow cavities. Table 3.1 outlines domain geometry for each case. Figure 3.2 shows where the cases to be studied lie with respect to the geometries tested by Vincent.

3.3   Grid

As a result of Casey's [2] observation that a laminar flow solver is sufficient to capture flow dynamics inside the dimple and necessary to model sparation, no turbulence model was used for this investigation. This greatly reduces the computing cost by requiring fewer equations to be solved and by reducing the required size of the grid. However, in order to assure that the grid is not too coarse to capture important flow characteristics, grid spacing adjacent to the wall, yp, is set to:

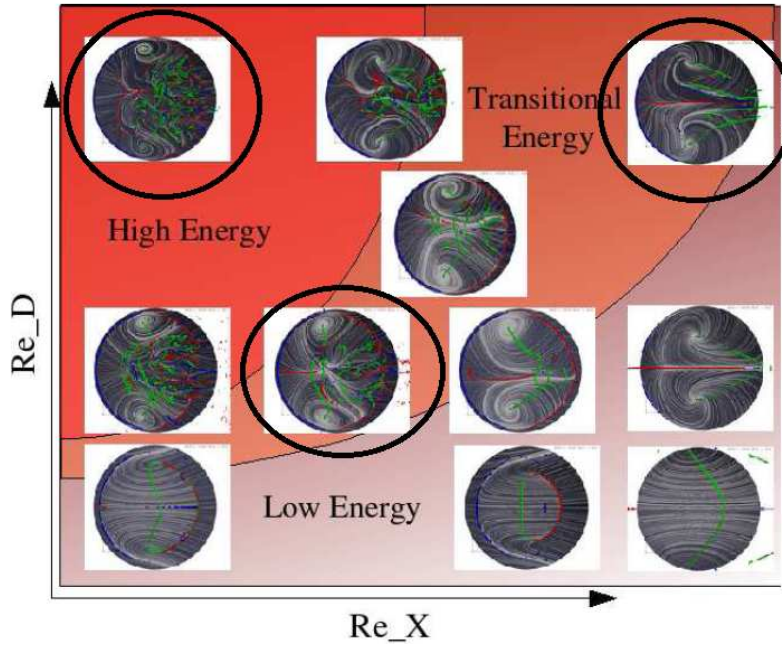$$y_p\sqrt{\frac{U_\infty}{\nu x}} \leq 1.0 \qquad (3.2)$$

Figure 3.2:   The range of geometries tested by Vincent, with the ones to be studied in this investigation circled in black [14]

This gives a limit of $1.05e^{-4}$m for the initial vertical cell spacing.

This investigation used Vincent's grids modified to vary dimple depth, and so the grid topology is very similar to Vincent's. In order to get more cells into the dimple, Vincent reduced the cell spacing there. Vincent used a hyperbolic tangent function with an initial spacing of 5E-6m for the cell spacing in the dimple. The final grid had 240 nodes on the dimple perimeter, 3400 horizontally across its interior, and 35 in its depth for a total of about 121,000 cells in the dimple. In the streamwise direction, Vincent stretched and compressed the dimple spacing to maximize resolution for a distance of two dimple diameters upstream of the dimple and three dimple diameters downstream.

Vincent's grids each consisted of 18 blocks. The total length and size of each grid depended upon Re_D and Re_x of the particular case. For this investigation, three of Vincent's grids were modified. These grids corresponded to the Re_D and Re_x for which dimple depth was varied. The grids originally contained a dimple with a depth
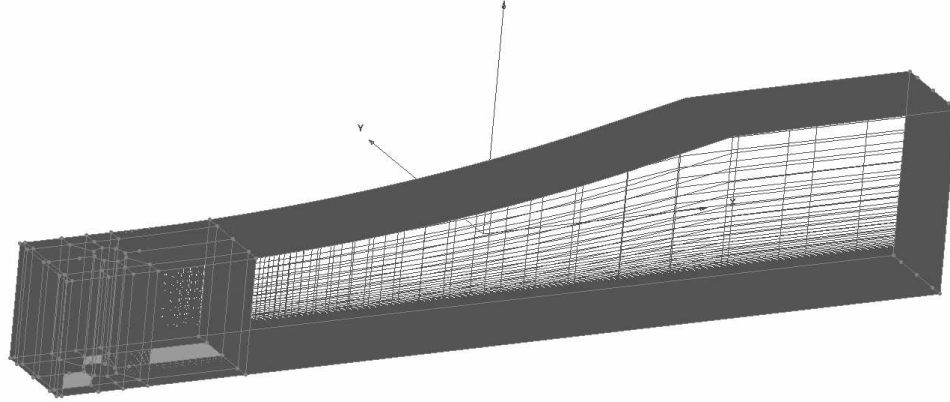
16

Figure 3.3:   Typical grid layout

to diameter ratio of 0.1. In order to change this ratio to that needed for each case of the investigation, the dimple grid was projected onto a section of a sphere with size and location necessary to produce a dimple of the desired depth. This gave spherical dimples of the same diameter and grid topology as those produced by Vincent. The total number of cells varied with the size of the grid; for the smallest case (Re_D of 9500, Re_x 21000) the total number of cells is 1.64 million and for the largest case (Re_D of 20500 Re_x 5000) the total number of cells is 3.17 million.

Figure 3.3 and Figure 3.4 show several views of the Re_D 9500, Re_x 21000 grid with dimple depth to diameter ratio of 0.15. The grids for the different cases are generally similar. For changing Re_x, the dimple is moved in the streamwise direction. For changing Re_D, the dimple diameter (and thus overall width of the domain) is increased.

3.4   Flow Solver

Fluent was the CFD solver used in this investigation. Fluent [4] is a control volume based flow solver. It functions by transforming the governing equations for mass and momentum (Equations 3.4 and 3.5) into discretized algebraic equations. It

17
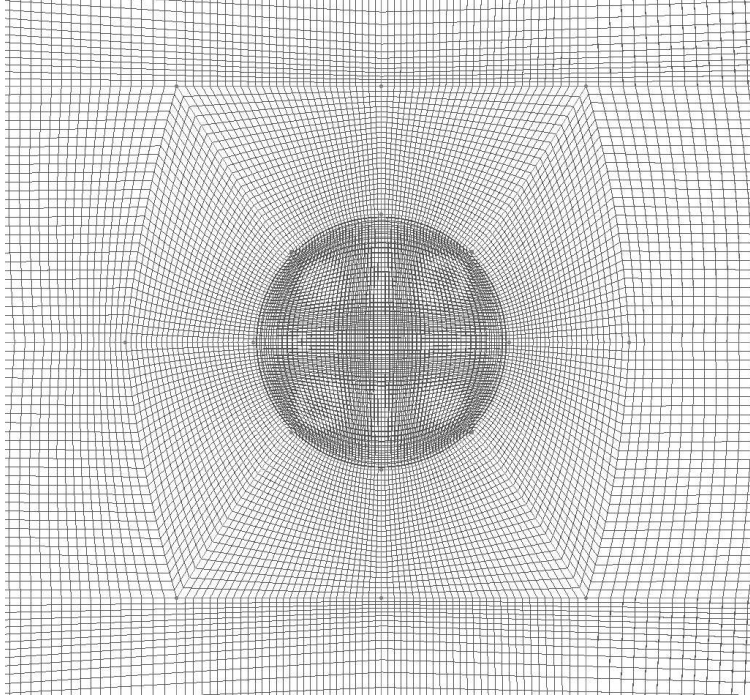
Figure 3.4:   Closeup view of the dimple

then linearizes these equations to obtain a solution to update the variables.

$$\frac{\delta \rho}{\delta t} + \nabla \cdot (\rho \vec{v}) = S_m \tag{3.3}$$

$$\frac{\delta}{\delta t}(\rho \vec{v}) + \nabla \cdot (\rho \vec{v} \vec{v}) = -\nabla p + \nabla \cdot (\overline{\overline{\tau}}) + \rho \vec{g} + \vec{F} \tag{3.4}$$

Fluent applies the above differential equations to the domain using a control volume approach. The governing equations are integrated about a control volume to give

discrete conservation equations in each control volume; the following is an example.

$$\oint \rho\phi\vec{v} \cdot d\vec{A} = \oint \Gamma_\phi \nabla\phi \cdot d\vec{A} + \int_V S_\phi dV$$

where

$$
\begin{aligned}
\rho &= \text{density} \\
\vec{v} &= \text{velocity vector} \\
\vec{A} &= \text{surface area vector} \\
\Gamma_\phi &= \text{diffusion coefficient for } \phi \\
\nabla\phi &= \text{gradient of } \phi \\
S_\phi &= \text{source of } \phi \text{ per unit volume}
\end{aligned}
$$

This equation is applied to each cell in the domain. The resulting variable value is stored at each cell center. However, face values are required to update variable values at each cell. Different interpolation techniques used are described below.

The flow velocity for this investigation is 10 m/s. A flow velocity this low is well within the incompressible regime, and density will be nearly constant. Because of the low speed flow, a segregated solver is used in which the governing equations for mass and momentum are solved sequentially. In the segregated solver, the continuity equation is used as a pressure equation. In order to introduce pressure into the continuity equation, the Semi-Implict Method for Pressure-Linked Equations (SIMPLE) is used.

The SIMPLE scheme relates pressure and velocity corrections to calculate the pressure field and ensure conservation of mass. It starts by solving the momentum equation with a guessed pressure field

$$J_f^* = \hat{J}_f^* + d_f(p_{x0}^* - p_{c1}^*) \tag{3.5}$$

However, the result does not satisfy continuity. In order to correct this, a fluctuation as a function of pressure is added to the face flux

$$J'_f = d_f(p'_{c0} - p'_{c1}) \tag{3.6}$$

with p' a cell pressure correction term. The flux correction equations are then substituted into the continuity equation to solve for cell pressure correction

$$a_P p' = \sum_{nb} a_{nb} p'_{nb} + b \tag{3.7}$$

with b the net flow rate into the cell

$$b = \sum_f^{N_{faces}} J^*_f A_f \tag{3.8}$$

This pressure correction is multiplied by an under-relaxation factor and added to the guessed pressure.

Pressure is stored at cell centers. However, the discritzed momentum equations require pressure values at cell faces. For this investigation, a second order interpolation between cell centers is used to obtain pressure on cell faces. The second order scheme is used to provide greater accuracy in the complex vortical flows. The interpolation is based on a Taylor expansion of the solution at the cell center about the centriod of the cell

$$\phi_f = \phi + \nabla\phi \cdot \Delta\vec{s} \tag{3.9}$$

with $\Delta\vec{s}$ as the displacement vector from the upstream centroid to the face centriod, and ϕ and $\nabla\phi$ are the cell centered value and its gradient. The gradient value is found using a discrete form of the divergence theorem

$$\nabla\phi = \frac{1}{V} \sum_f^{N_{faces}} \tilde{\phi}_f \vec{A} \tag{3.10}$$

20

A higher order momentum interpolation is used for this investigation, again to better capture the complex vortical flows in and beyond the dimple. For momentum, a third-order MUSCL (Monotone Upstream-Centered Schemes for Conservation Laws) scheme is used. This scheme combines a second order upwind scheme with a central difference scheme.

$$\phi_f = \theta\overline{\phi} + (1-\theta)\phi_{f,SOU} \tag{3.11}$$

In Equation 3.12, ϕ_f is the center face value of ϕ, and $\phi_{f,SOU}$ is that value computed with the second order upwind scheme. The basic MUSCL approach is based upon using a hybrid scheme to find the values to the left and right of a face of interest. Blazek [1] gives the following equations:

$$
\begin{aligned}
U_R &= U_{I+1} - \frac{\epsilon}{4}[(1+\hat{k})\Delta_- + (1-\hat{k})\Delta_+]U_{I+1} \\
U_L &= U_I - \frac{\epsilon}{4}[(1+\hat{k})\Delta_+ + (1-\hat{k})\Delta_-]U_I
\end{aligned}
$$

where U_R is the right state (i.e. state beyond face of interest) and U_L is the left state. The parameter $\hat{k}$ affects the balance of the interpolation. Different values of $\hat{k}$ will result in different interpolation types. For example, if $\hat{k}=1$, then MUSCL reduces to a central scheme, if $\hat{k}=1/3$, MUSCL will be a third order scheme.

3.4.1 Boundary Conditions. The boundary conditions were the same for each geometry tested. The front wall is a velocity inlet of 10 m/s. The rear wall is a velocity outlet. The side walls are periodic. The top wall is a slip surface with zero shear stress. The bottom wall and dimple are no-slip walls.

3.5 Data Collection and Flow Visualization

In each case studied, seven monitors were placed with equal spacing between the center of the dimple and the end of the domain. These monitors were set to record static pressure at each time step. The pressure taps are useful for gauging and comparing flow activity in and downstream of the dimple. The power spectrum of

Table 3.2: Streamwise location of the pressure taps in each case (in cm), where the first pressure tap is centered above the dimple

Re_D/Re_x	Tap 1	Tap 2	Tap 3	Tap 4	Tap 5	Tap 6	Tap 7
9000/21000	-2.99	2.92	7.58	12.86	18.15	23.43	34.00
20500/5000	-0.01	4.85	9.71	14.57	19.42	24.28	34.00
20500/77000	6.60	10.52	14.43	18.34	22.26	26.17	34.00

the pressure tap is used to find possible dominant frequencies. Table 3.2 gives exact pressure tap locations for each case.

The prevalence of unsteady vortical structures in this investigation results in a time-dependent problem, calling for an unsteady computation. A time step size of $1 * 10^{-4}$ was chosen as a balance between problem stability and computing cost. Collecting data on the entire grid often enough to resolve flow characteristics is not possible (one data file is about 300-500 Megabytes; scores of data files for each of the 8 cases would be required). In place of Fluent's data exporter, a VTK Extractor was used. For each case, a box was established around the dimple for runtime data export to a Visualization Tool Kit (VTK) XML file. Each box consisted of, roughly, a domain starting one-half dimple diameter upwind of the dimple to one diameter behind, one dimple diameter across, and from the floor of the dimple to one half diameter above the dimple. Specific box geometry varied for each case to minimize box size while ensuring that all pertinent flow characteristics were included.

VTK is a 3D visualization application available freely. It is capable of facilitating visualization of scalars, vectors, and tensors, making it very flexible and powerful in analyzing CFD data [11]. The Fluent VTK Extractor (FVE) used here was developed specifically to save a portion of the Fluent data generated at runtime [8]. FVE uses the grid manipulation, sampling, and input/output capabilities of VTK. It is implemented through the use of two user defined functions in Fluent. The first function defines the bounding box and the data (i.e., velocity, pressure, density, etc.) to be exported. The other function writes the desired data at specified time steps. The functions and the

FVE libraries are built and loaded into Fluent. Fluent then calls these FVE functions at runtime and exports data as instructed. For this investigation, data is exported every 10 time steps. For this incompressible flow case, components of velocity are sufficient for evaluating any parameter of interest, and so are the only quantities exported with FVE.

Ensight 8 is used for flow visualization. Ensight [3] groups elements of a model into parts. Different operations can be applied to each part for a wide variety of flow characteristics and visualization settings. Ensight can easily handle time-dependent data, important for this unsteady flow problem. Other principle features of insight to be used include particle traces, vortex cores, vorticity isosurfaces, and velocity vectors.

Particle traces are extremely helpful in qualitative flow analysis. Particle traces are made by a time integration of a vector field variable using a fourth order Runge-Kutta method with a time varying integration step. Integration can be restricted by specifying which vector components to use. For example, surface restricted traces may be made by using only the velocity component tangent to the surface. Particle traces are used for surface flows on the dimple itself and to observe the behavior of flow through and above the dimple. For the former, 300-400 sources are placed within the dimple and constrained to move on the dimple surface. For the latter, a rake is placed upstream of the dimple just above (on the order of 0.1mm) the domain surface. From this rake are emmited 20-50 evenly spaced streamlines.

Vortical motion is a dominant feature of the flow in this investigation; it is the vortices that are thought to make the dimples effective in alleviating separation. Thus, their behavior will be of great interest. The strength, location, movement, and endurance of the vortices are examined. This will require identification of vortex cores. Ensight uses the velocity gradient tensor of a three dimensional flow field to locate vortex core segments. Vortex cores are computed using an algorithm based on critical point theory [12]. A critical point of a vector field is one where the vector

magnitude vanishes. If the rate of deformation tensor at a critical point has one real and one complex pair of eigenvalues, then the flow forms a spiral at that point with the real eigenvalue pointing in the direction about which the flow spirals. If a non-critical point has the necessary eigenvalues, the velocity in the direction of the real eignvalue is subtracted; if the resulting value is zero, then the point is the center of swirling flow. Algorithms developed by Sujudi, Haimes, and Kenwright are used in Ensight to calculate vortex cores [3].

Vorticity isosurfaces are also used to study the flow within the dimple. These surfaces are easily made based on calculating the curl of the vector field inside the domain. The vorticity isosurfaces are classified as low, medium, or high strength relative to each individual dimple. The high strength vorticity isosurfaces reflect vorticities that exist in small regions of the dimple, medium strength vorticity isosurfaces in more of the dimple (filling 30%-40% of the shear layer) and low strength vorticity isosurfaces exist throughout the shear layer and into the wake region. These vorticity isosurfaces help in making qualitiative comparisons of different dimple flow structures rather than quantitative comparisons of vortex strength.

As this is a principally qualitative investigation, the structure, trends, and patterns of flow within each dimple are the main characteristics studied. To this end, for each dimple case, animations are made from the data collected for each dimple. The animations include surface oil flows on the dimple itself, vortex cores, velocity profiles, separation and reattachment lines, streamlines and vorticity isosurfaces. From these animations comparisons are made between the flow structure of different dimples (each of the nine different dimples), cases (the 3 different Re_D Re_x combinations studied), and categories (groupings based upon flow structure, explained in Chapter 4).

IV. Results

While each dimple geometry investigated had its own unique characteristics, the dimples fell into four general categories of flow. These categories are identified by general names according to their overall structure and characteristics. These categories do not reflect definite, near-identical groups of dimples; rather, they provide a means of guiding analysis and serve to qualitatively group dimples. Table 4.1 gives an overview of the different geometries and the categories they fall into.

The categories are determined by character of flow within the dimple. In general, the steady category is distinguished by its fixed vortex activity and lack of significant time-dependent flow qualities. The quasi-steady category is characterized by the presences of dynamic pinned vortices revealed by oil flow surface sinks. The bulk shed category is marked by many of the same features as the quasi-steady, except with occasional large-scale shedding and disruption of dimple flow. The chaotic category is characterized by little observed structure or regular motion associated with the bulk shed or quasi steady flow cases. More characteristics of each category are described in their respective sections below, along with details of the sometimes significant differences between different dimples within the same category. Comparisons to Vincent's observations for each dimple are also given.

Table 4.1:   Category of each dimple

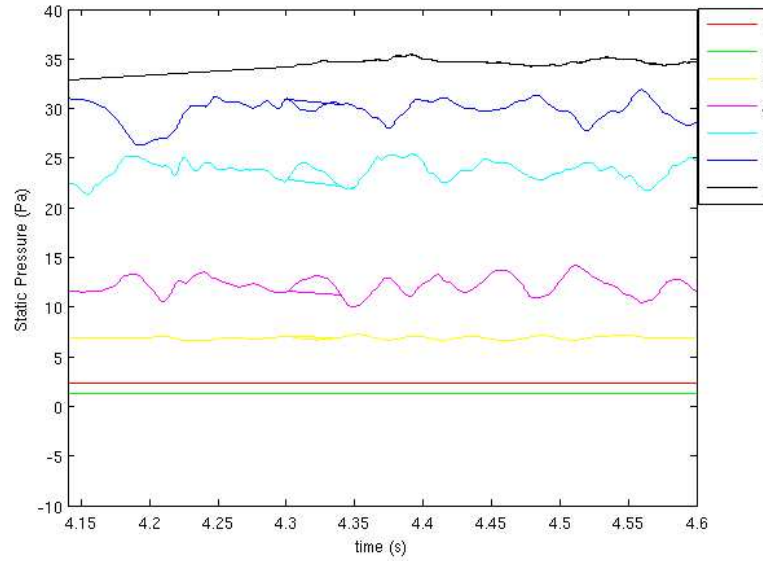| Re_D	Re_x	Depth to Diameter Ratio	Flow Category
9000	21000	0.05	Steady
20500	5000	0.05	Steady
20500	77000	0.05	Steady
9000	21000	0.25	Quasi-Steady
20500	77000	0.15	Quasi-Steady
9000	21000	0.15	Bulk Shed
20500	5000	0.15	Chaotic

Figure 4.1:   Pressure variations recorded for Re_D 9500, Re_x 21000 0.05 h/D Dimple

4.1 Steady Category

All three 0.05 dimple depth to diameter ratio cases showed near steady behavior. There is little vortical activity, and pressure tap data for all three of these cases is strikingly similar. Figure 4.1 shows a typical plot of pressure tap data. The first two pressure taps show no activity; pressure did not vary at all at the two pressure taps directly above and just downstream of the dimple. It varied only little in the pressure taps further downstream. The behavior of the first pressure tap suggests essentially no time-varying activity within the dimple for all dimples within this category. Assuming this suggests that the activity of the downstream pressure taps is not a result of the dimple. The activity at these taps is most likely due to flow disturbances resulting from separation. Examination of the separation location corroborates this; the second (and last calm) pressure tap is located just downstream of the separation line. Taps further downstream are within the region where the flow has separated.

The PSD plot (Figure 4.2) of the pressure tap data is also similar for all three of these cases. Again, there is little power spectrum activity in the first two pressure taps, confirming that the flow by these two stations is nearly steady. As with the pressure
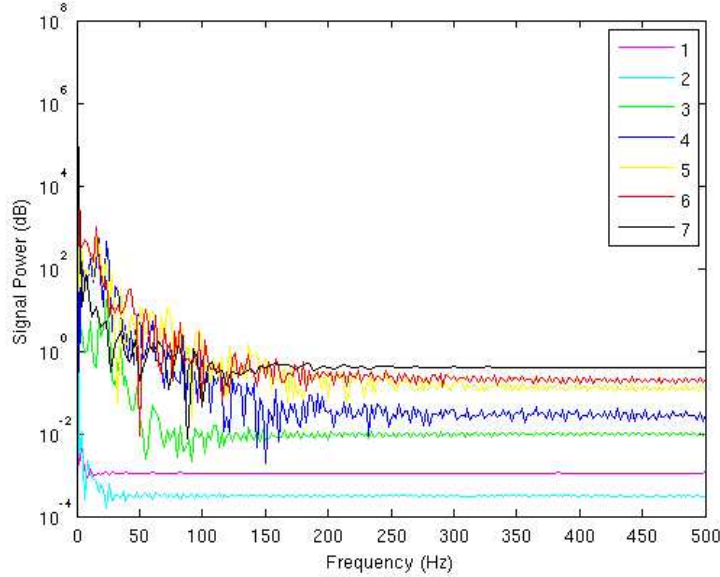
26

Figure 4.2:   PSD plot of pressure tap data for Re_D 9500, Re_x 21000, 0.05 h/D Dimple

taps, this conclusion suggests that the frequencies observed in the downstream taps are a result of disturbances associated with separation, and not from dimple activity.

The streamlines, vorticity isosurfaces, oil flows, and velocity vector profiles provide more detail in the dimple flow and, for each dimple, corroborate general conclusions drawn from the pressure tap and PSD data. When animated, they show almost no time-dependent change. Figure 4.3 shows oil flow and streamlines typical for this category. The lack of dimple effect on the streamlines, emitted from just above the domain surface upstream of the dimple, is clear.

Despite the overall similarity between these cases, close examination of the flow dynamics within these dimples reveal that they are not the exact similar, whatever the overall effect on the flow may be. Figure 4.4 compares the velocity profile typical of the Re_D 9000 Re_x 21000 dimple (which is very similar to the Re_D 20500 Re_x 77000) to the velocity profile of the Re_D 20500 Re_x 5000 dimple. The higher Re_x dimples both contain a large fixed spanwise vortex in the middle of the dimple, as evident in the velocity profile. Surface flows and separation lines reveal this vortex results
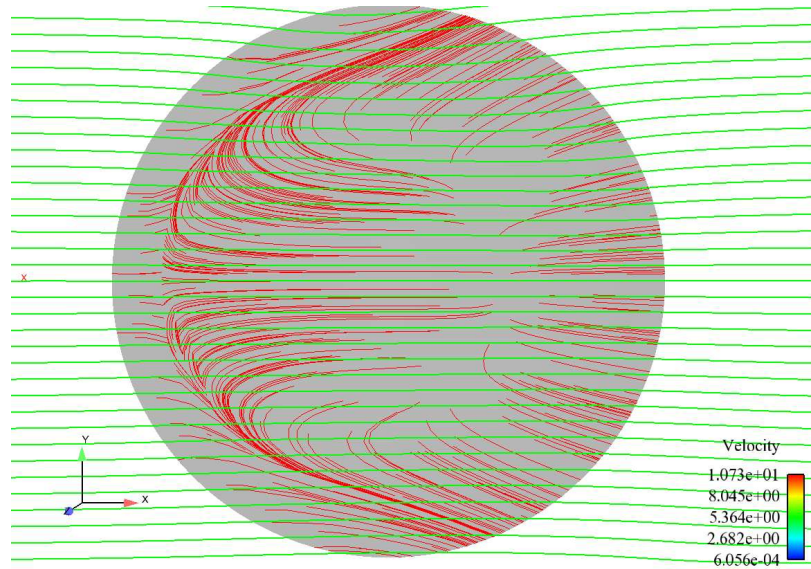
27

Figure 4.3:   Surface line (red) and channel streamlines (green) of the Re$_\mathrm{D}$ 9500 Re$_\mathrm{x}$ 21000 dimple

in a separation line near the dimple leading edge and attachment line in the back half of the dimple. The remaining case, however, shows slightly different behavior. The region of reversed flow within the dimple is much smaller, and is located on the slope on the upstream half of the dimple. Examination of boundary layer thickness compared to dimple depth may provide an explanation for this.

As shown in table 4.2, the two cases with standing vortices have a dimple depth less than boundary layer thickness, while the case with a much smaller vortex and region of reversed flow has a dimple depth much greater than boundary layer thickness. This results in freestream air being drawn deeper into the dimple. The presence of higher velocity air closer to the surface is likely helping to prevent reversed flow on the dimple. This reveals that the depth of the dimple in relation to the thickness of the boundary layer can affact dimple flow behavior.

These dimples probably show little effect on the channel flow because they are not deep or steep enough to produce large velocity gradients. Vortices are essential to flow mixing, and vorticity is equal to the curl of the velocity field $\vec{\omega} = \vec{\nabla} \times \vec{V}$. If velocities and velocity gradients are small, vorticity will be small, and flow mixing will

28
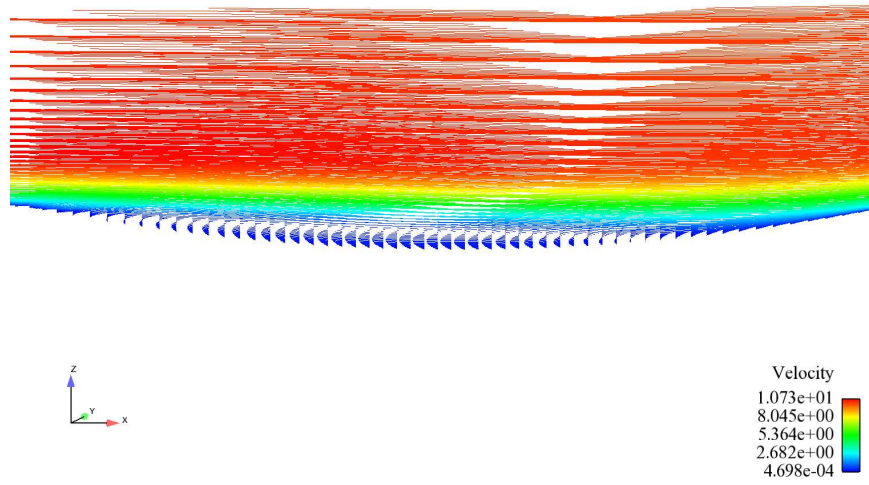
(a)
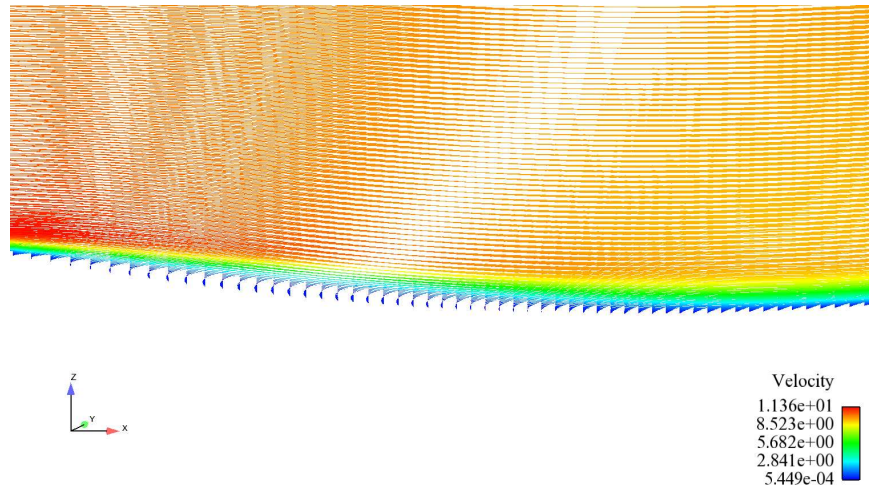
(b)

Figure 4.4:   Velocity profiles of the (a) Re_D 9000 Re_x 21000 (b) Re_D 20500 Re_x 5000 dimple

Table 4.2:   Comparison of dimple depth and boundary layer thickness among dimples of the steady category

Re_x	Dimple Depth (cm)	δ^*_{99} (cm)
5000	0.150	0.045
21000	0.069	0.089
77000	0.150	0.22

be minimal. These dimples have gradual depth changes and small velocity gradients. While dimple flow in general is much more complicated than this, the explanation should be sufficient for this particular shallow geometry.

4.1.1 Comparison with Vincent. Even though the lack of activty may make this category seem uninteresting, the absence of effect on the flow has signficiant implications. All cases showed behavior for a 0.05 depth to diameter ratio (h/D) dimple that differed greatly from Vincent's depth to diameter ratio of 0.1. The difference in the Re_D 20500 Re_x 5000 case is especially apparent. Vincent's 0.1 depth to diameter ratio dimple for this case showed highly chaotic, highly random behavior. Vincent's dimples for the other cases show pinned horseshoe vortices rather than a fixed separation bubble. Each 0.05 depth to diameter ratio dimple, however, acted much like the others of similar depth to diameter ratio. These shallow dimples behave much more like Vincent's small diameter/low Re_D cases (Figure 4.5). The stark differences between the 0.05 diameter dimples and the 0.10 reveal that dimple depth does have an effect on dimple flow.

4.2 Quasi-Steady Category

This category (the 0.15 h/D Re_D 20500 Re_x 77000 and 0.25 h/D Re_D 9500 Re_x 21000 dimples) shows much more impact of the dimple on the flow than the steady category. The pressure tap data (Figure 4.6) for the dimples within this category show at least some degree of activity (however small) in the first pressure taps where it was lacking in the steady category. This suggests more flow activity within the dimple. While the 0.25 h/D dimple does not show much activity through 2.3 seconds, there is a continual, if small, pressure variation at all taps by 2.35 seconds. The 0.15 h/D dimple shows much more activity throughout the time domain. However, this downstream activity gradually dampens as the flow moves downstream.

The PSD data (figure 4.7) from these cases show less similarity. The PSD plot for the 0.25 h/D case resembles the steady category PSD plots; it begins with a high
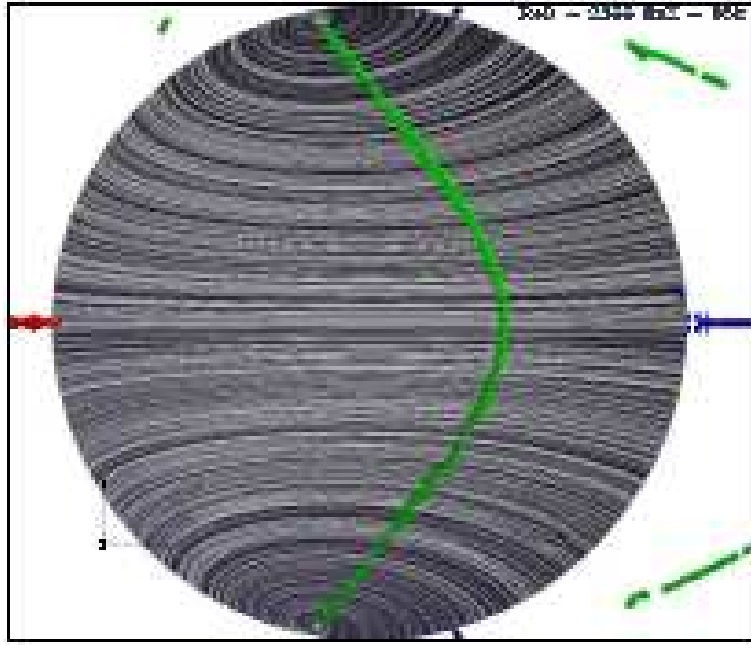
Figure 4.5:   Vincent's 0.10 depth to diameter ratio dimple of Re_D 2500 and Re_x 95000

signal power, then quickly drops off leaving little but noise at higher frequencies. The only two possible candidates for distinct frequency peaks are at about 100 Hz and 400 Hz; however, these peaks are small and not very distinct. In contrast to the steady category PSD plots, the 0.25 h/D dimple retains high frequency activity above and just downstream of the dimple as the taps further downstream show less. The 0.15 h/D case, on the other hand, has a distinct spike at 400 Hz. There is significant spectrum activity throughout the frequency range for the first several taps. As with the 0.25 h/D dimple, though, the pressure taps towards the end of the domain show little activity beyond 200 Hz. While it may seem that the pressure tap and PSD data make these two dimples appear more different than similar, it was not for the pressure tap and PSD plots that these two cases were grouped together.

Surface oil flow plots (figure 4.8) reveal interesting similarities between these two cases. Both contain two distinct surface sinks on either side of the chordwise centerline. In each case, these surface sinks form near the rear of the dimple and
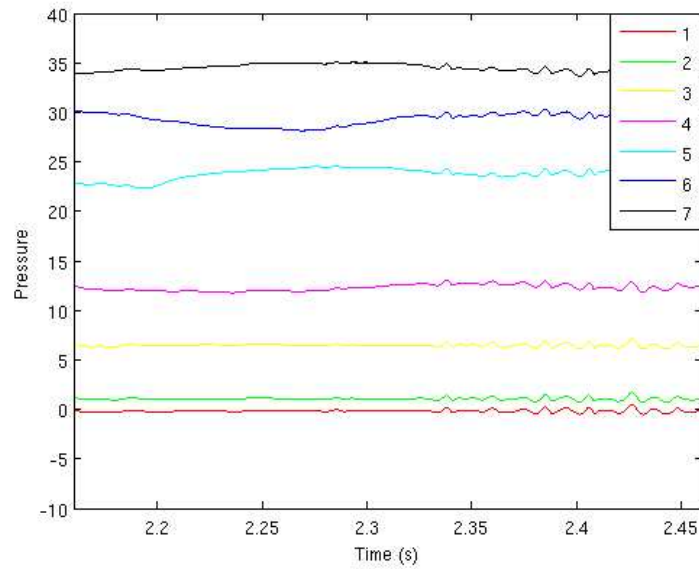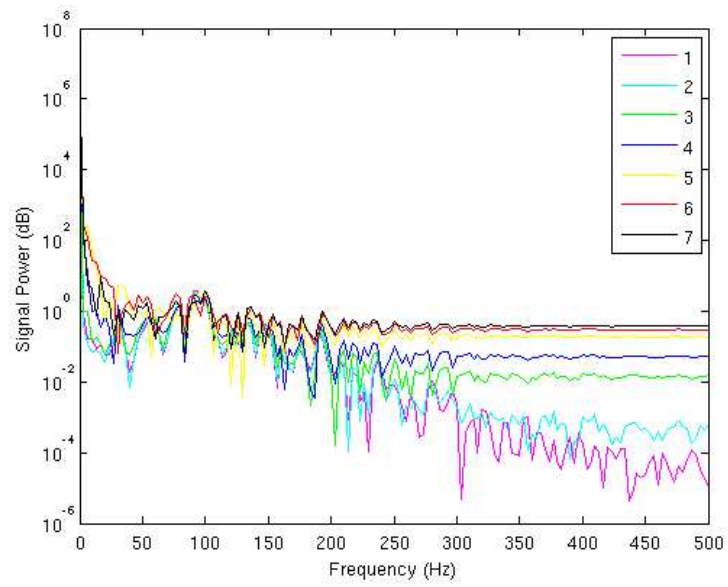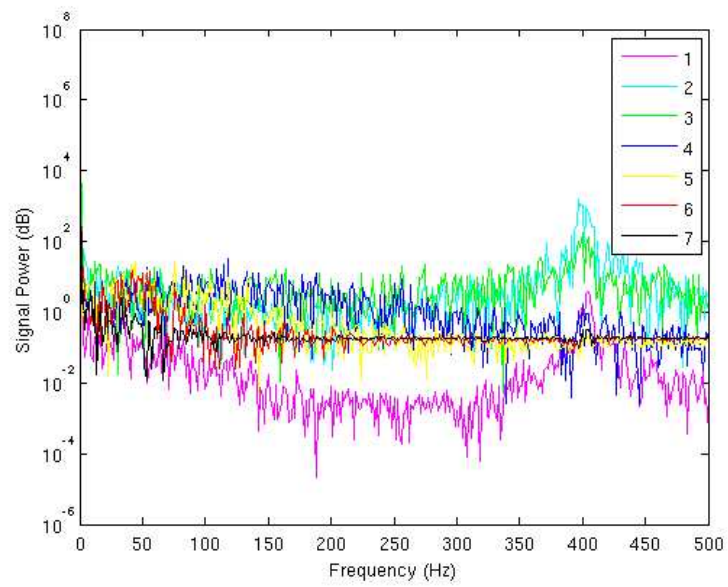
(a)
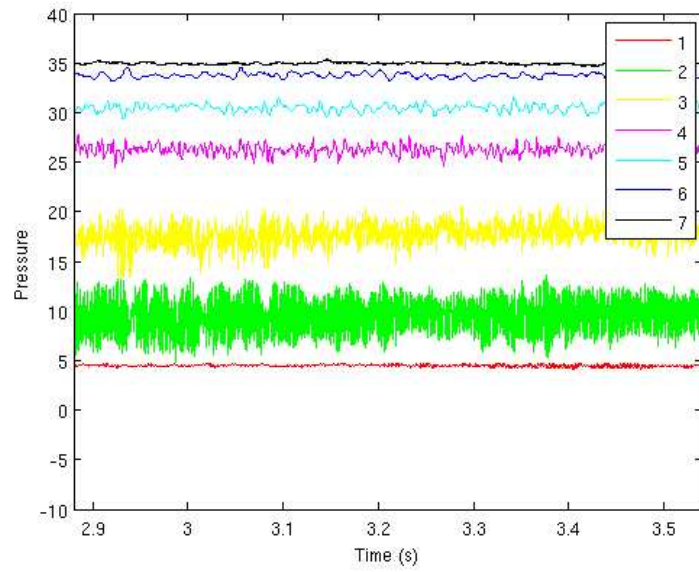
(b)

Figure 4.6:   Pressure tap data for each of the 7 pressure taps (a) 0.25 h/D dimple (b) 0.15 h/D dimple

(a)

(b)

Figure 4.7: PSD for each of the 7 pressure taps (a) 0.25 dimple (b) 0.15 dimple

move upstream towards the front of the dimple. Visualization of vortex cores reveals that each of these sinks is the site of a pinned vortex core. The vortex cores appear to trace vortices up through the dimple and turn spanwise as they reach the shear layer. Each of the surface sinks tends to wander in the areas denoted in parts a and b of Figure 4.8. The regions of vortex wandering are fairly similar. In the aft section of the dimple, a region of disorganized surface lines is present. This area corresponds to the wake region observed by Vincent [14], shown in Figure 2.2.

Despite the similarities, the behavior of the pinned vortices does differ in some respects between the two cases. For the 0.25 h/D dimple, the sinks begin fairly disparate and gradually coalesce into two co-existent vortex cores. The development of these sinks begins in the rear of the dimple, in the wake region. Both begin to develop at the same time. As they develop they move upstream in the dimple and are able to remain fixed even slightly above the spanwise centerline of the dimple. The sinks (and associated pinned vortices) coalesce at about the same time as the pressure flucuations observed in the pressure tap data (figure 4.6) begin. The sinks for the 0.15 dimple are far more dynamic; they continually form in the wake region, move upstream, and break up after passing into the front half of the dimple. Usually, only one sink is present at a time. The formation and dissipation of the sinks in this case shows almost alternating behavior; usually one sink develops as the other dissipates.

The velocity profiles (Figure 4.9) reveal two interesting details about the flow through these dimples. First, the velocity magnitude in the dimple below the shear layer is small for each dimple except in the wake region in the rear of the dimple. The velocity for both dimples seems to be fairly uniform reversed flow in the depths of each dimple. This suggests that much of the activity in the dimple occurs along the shear layer across the mouth of the dimple and in the wake region in the rear of the dimple. This is supported by a profile inspection of vorticity isosurfaces (Figure 4.10). Secondly, regions of high vorticity are concentrated in the shear layer and in the wake region as described by Vincent [14]. Much lower magnitudes of vorticity are observed
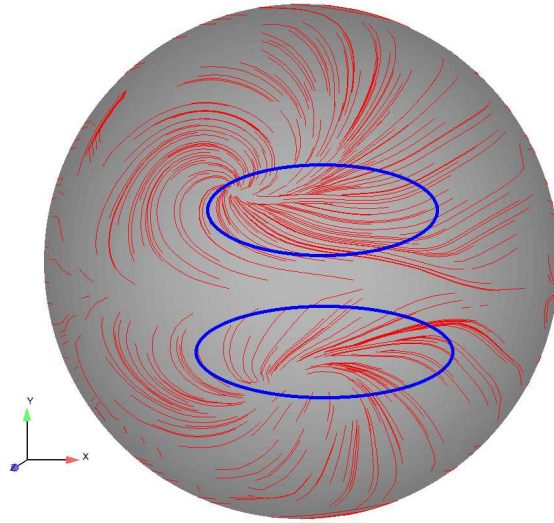
(a)
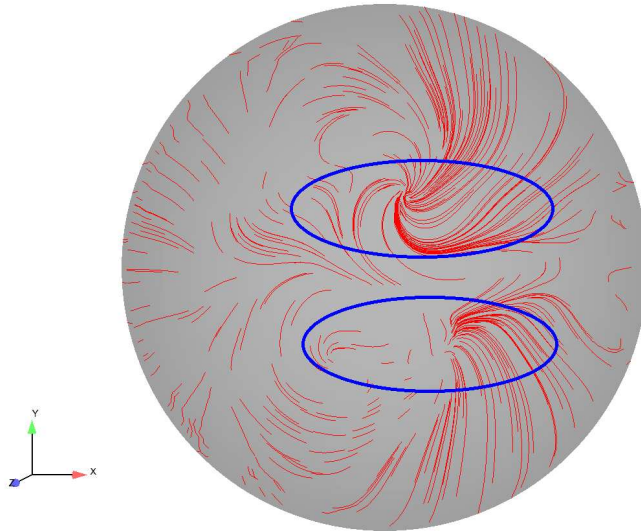
(b)

Figure 4.8:   Typical surface flow for quasi-steady category with general areas of sink movement circled in blue (a) 0.25 h/D dimple (b) 0.15 h/D dimple

within the dimple itself. The velocity profiles also provide an explanation for the forward movement of the dimples. The flow near the dimple bottom is reversed, which would pull the surface sinks upstream. The velocity profiles also give greater detail on the wake regions; large vortices fill the wake region, as revealed by the swirling flow in the rear of the dimple.

Unlike in the steady category, a variety of vortical motion is present in both these dimples. In addition to the pinned vortices at the surface sinks, there also exist streamwise vortices in the wake region and spanwise vortices in other regions of both dimples. Figure 4.11 below shows a significant feature revealed by vorticity isosurfaces, the existence of a vortex "heart" near the center of the dimple. The heart consists of a distinct group of medium vorticity isosurfaces just upstream of the center of the dimple. This heart was present in both dimples, though in the 0.25 dimple, it did not appear until the pinned vortices had developed. The streamwise vortices in the wake region and the vortices shed by both dimples appeared to originate from this heart. The velocity profiles (Figure 4.9) reveal that this region of vorticity likely results from a maximum velocity gradient above the center of the dimple. Behind the center of the dimple is the wake region, with more distinct vorticies but smaller gradients, hence lower strength vorticity isosurfaces. The vortices shed by the hearts, however, are often quite strong. These regions of high vorticity emerge as the pinned vortices are able to interact with the heart and produce greater shedding.

There appears to be an association between the streamwise vortices (or streamwise elements of spanwise vortices) and the sinks revealed by the surface flow. The dominant spanwise vortices may originate from the bow of the dimple as flow curves down into the dimple and is pulled downstream. The sink flows appear to largely draw flow from the sides of the dimple and then project up and inwards towards the middle of the dimple (Figure 4.12). These trends reflect the description of flow offered by Ligrani [7]. The flow projected upwards from the sink is swirling due to the curve of the dimple sides, and is pulled downstream by the bulk flow.
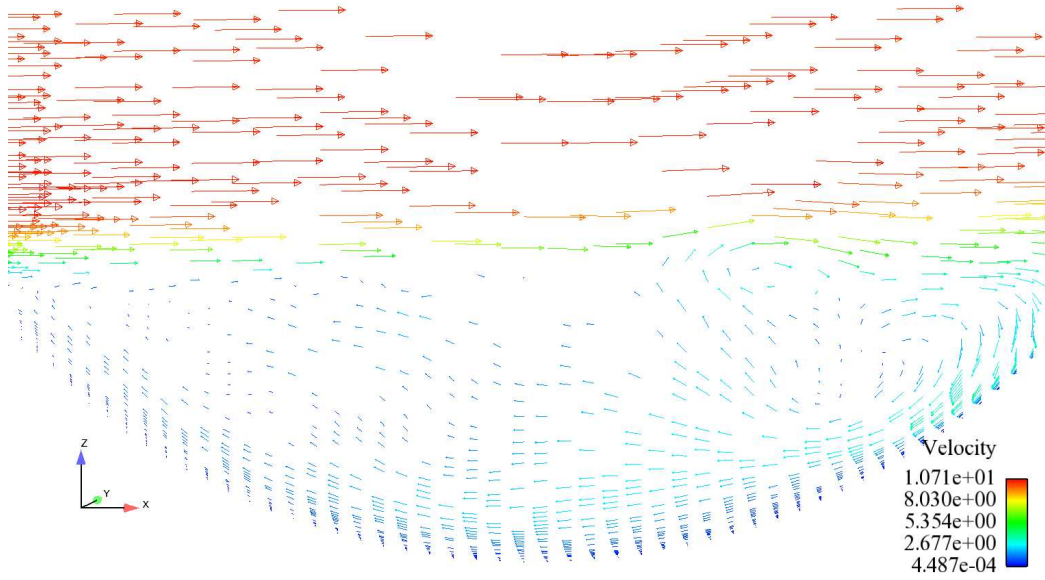
(a)
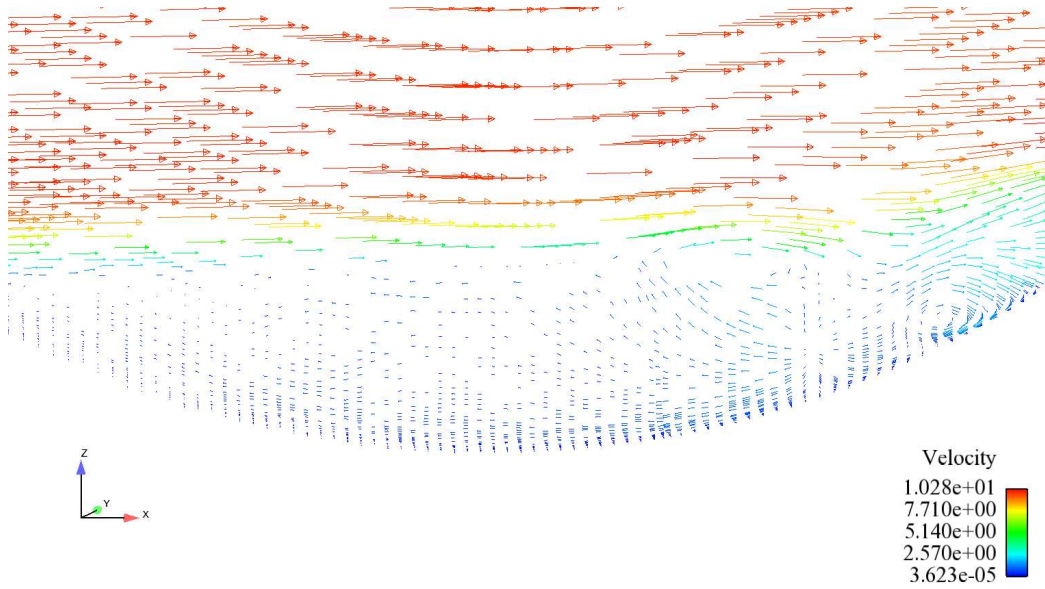
(b)

Figure 4.9:   Typical centerline velocity profiles for quasi-steady dimples (a) 0.25 h/D dimple (b) 0.15 h/D dimple
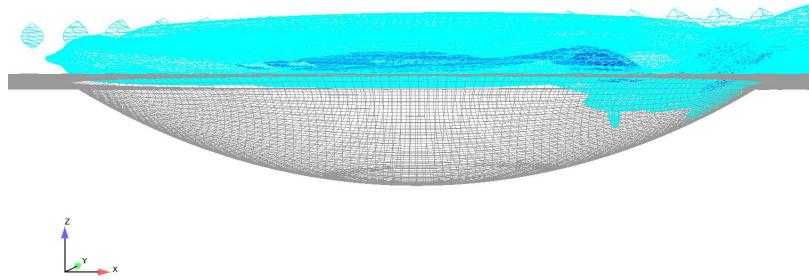
Figure 4.10:   Vorticity isosurfaces in 0.15 h/D dimple with medium strength in light blue and high strength in dark blue
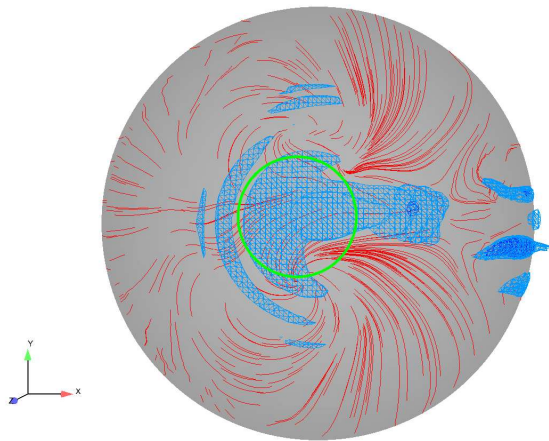

Figure 4.11:   0.15 h/D dimple with vorticity heart circled in green
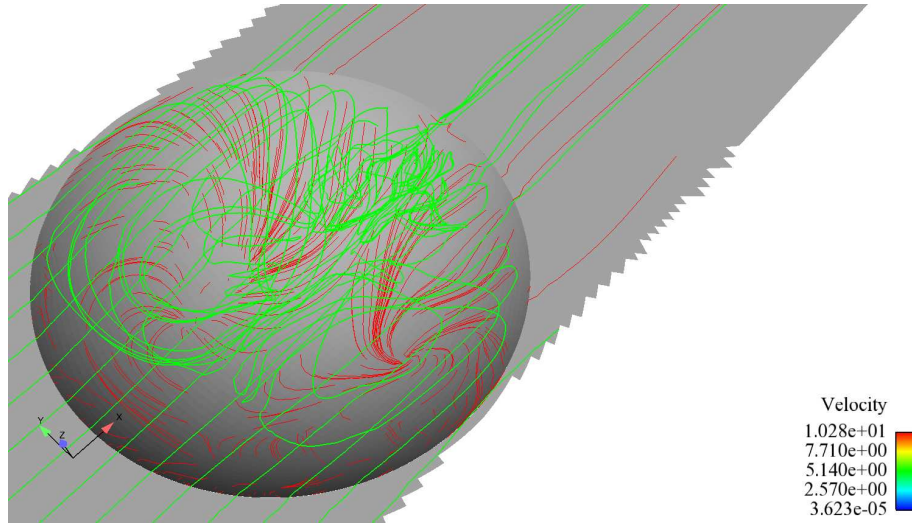
Figure 4.12:   Green streamlines are drawn in the sides of the dimple into vortices pinned at the surface sinks

The shedding of vortices also strongly differentiates these two cases. The pressure taps and vorticity isosurface data for the 0.25 h/D case suggest that few significant pressure waves are produced and few strong vortices are shed past the dimple. However, the 0.15 h/D case shows different behavior. Large regions of high strength vorticity impact the downstream surface of the dimple roughly every 2 or 3 timesteps, where the timestep size is 10e-4 s. This corroborates the PSD data suggesting a shedding frequency of 400 Hz. Low strength vorticity isosurfaces stretched streamwise downstream of the dimple. Vincent [14] identifies these vortices as beneficial in mitigating downstream separation.

Interestingly, the 0.15 h/D case has a greater total dimple depth than the 0.25 h/D case. However, it has a greater inlet area for its volume than the 0.25 h/D case. This suggests that dimple depth alone cannot be used to predict dimple flow characteristics; if greater dimple depth alone resulted in less vortex movement due to removal from high energy flow, then the total depth of the 0.15 h/D case would show less pinned vortex activity.

Examination of this category suggests that the motion of the pinned vortices may be a strong indicater of flow within the dimple. The 0.15 h/D case had continual

motion of pinned vortices and more downstream flow effects, in addition to a heart present throughout the time studied. The formation of the heart and fluctuation of pressure taps for the 0.25 h/D dimple occurred as the pinned vortices formed and moved forward, suggesting that the heart or pinned vortices at the sinks have a direct influence on downstream flow.

4.2.1 Comparison with Vincent. The flow in the 0.25 h/D dimple differed noticeably from the flow in the same case for Vincent's [14] 0.10 depth to diameter ratio dimple. While his dimple did contain pinned vortices moving in the dimple similar to the 0.25 dimple, these vortices, along with all the flow in the dimple, were subject to strong occasional disruptions, similar to the bulk shed case described later in this document. The 0.25 h/D dimple showed no such instability. The depth of the dimple may provide an explanation. Beneath the shear layer, as mentioned, much of the flow moves at a low velocity. The deeper 0.25 h/D dimple may be swallowing some of the vortical motion, particularly in the wake region. The extra depth may remove these flow features from the more dynamic environment at the shear layer.

The flow for the 0.25 h/D dimple somewhat resembles flow for a shallow cavity of equal depth to length ratio as observed by Grace [5] and Ozsoy [9]. In Ozsoy's and Grace's cavities there was a significant degree of flow activity within the cavity, but far less apparent activity downstream of the cavity. This is similar to the 0.25 h/D case. Despite the significant apparent activity within the dimple, the 0.25 h/D dimple seems to have little effect on the downstream flow, as suggested by the pressure tap data (Figure 4.6).

The flow in the 0.15 h/D dimple, on the other hand, behaved much like Vincent's 0.10 h/D dimple for the same case. Both had pinned vortices as revealed by surface sinks. In both of these dimples vortices were a stable feature; while they did move and alternatively disappear and re-form, their overall motion in the dimple was stable, as opposed to the bulk shedding case. The similarity here is interesting; the 0.15 h/D dimple is no closer in size to the 0.10 dimple than the 0.05 h/D dimple yet it shows

much more similar behavior. This suggests a "threshold" value for dimple depth which is able to produce sufficient velocity gradients to generate the pinned vortices and vortex heart.

The question remains as to why the 0.15 h/D dimple showed more downstream flow effects than the 0.25 h/D dimple. The swallowing explanation offered above may be useful here as well; many of the disturbances produced by the dimple remain in the dimple rather than escaping and moving downstream. Although the 0.15 h/D dimple has a greater total depth than the 0.25 h/D dimple, it also has a larger surface area. This may allow for a greater degree of flow mixing near the shear layer.

4.3   Bulk Shed Category

This case (the Re_D 9500 Re_x 21000 0.15 h/D dimple) showed interesting behavior; sort of a transition between quasi-steady and chaotic. It showed some traits of the quasi-steady case, but also had occasional bulk shedding where many of the vortical structures would be ejected from the dimple. The pressure taps (Figure 4.13) reveal several peaks at all tap locations. These peaks occur slightly later at each successive downstream location, suggesting a finite travel time of a pressure wave. The waves are most clear just above the dimple. The pressure variances are visible at the latter downstream pressure taps, but the pressure waves seems to dissipate as they reach the end of the domain. The buildup to each peak is quite similar in shape, suggesting similar behavior leading to each pressure peak. Also, after each peak, the return to small pressure variations occurs suddenly. Between these peaks there are variations in pressure, albiet smaller ones.

The PSD plot (Figure 4.14) shows two distinct peaks at about 500 Hz and 900 Hz. These peaks are most pronounced in the pressure tap immediately above the dimple; however they are evident in the further downstream pressure taps as well. Beyond the 1000 Hz range, most of the pressure taps quickly level off suggesting there is mostly noise at the higher frequencies. However, the two pressure taps nearest the dimple show definite activity out to the Nyquist limit (5000 Hz for the sampling
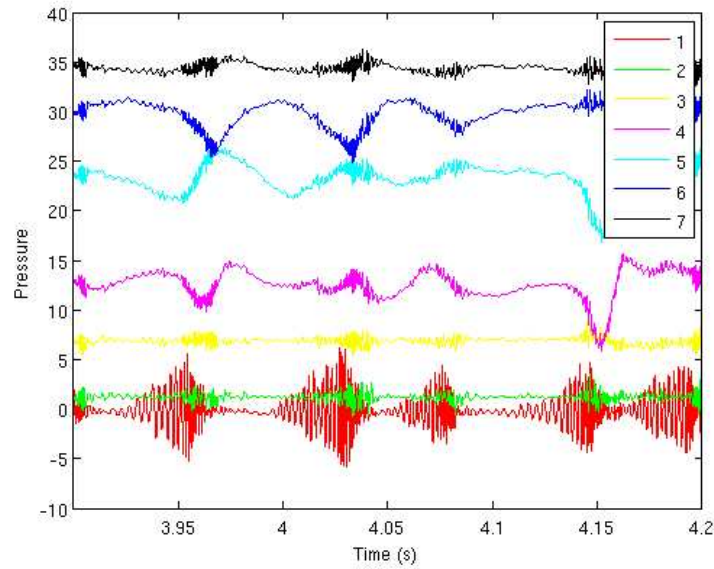
Figure 4.13:   Pressure tap data for each of the 7 pressure taps of the bulk shed dimple

rate of 10,000 Hz). This suggests significant high frequency activity within and just downstream of the dimple; however, this high frequency activity appears to have little effect on the downstream flow. Behavior above about 500 Hz is difficult to observe with a time step size of 1e-4, as this behavior takes place over less than two time steps.

A time accurate examination of oil flow lines, vorticity isosurfaces, and particle traces through the dimple reveal the flow tends to operate in alternating stable and unstable cycles. The terms "stable" and "unstable" are given to aide in discussion. At the beginning of a cycle, surface flow lines and vorticity isosurface reveal a pinned horseshoe vortex, similar to that observed in the quasi-steady category. Figure 4.15 shows surface oil flows and vortex cores typical of the stable period of flow. This figure also shows the pinned vortices at the oil flow sinks. As time progresses, the vortex location moves upstream inside the dimple. As the pin location approaches the midpoint of the dimple, the vortex appears to become unstable and large-scale shedding from the dimple occurs, as evidenced by the behavior of the pressure tap data (Figure 4.13). After a period of very chaotic flow activity with large movement
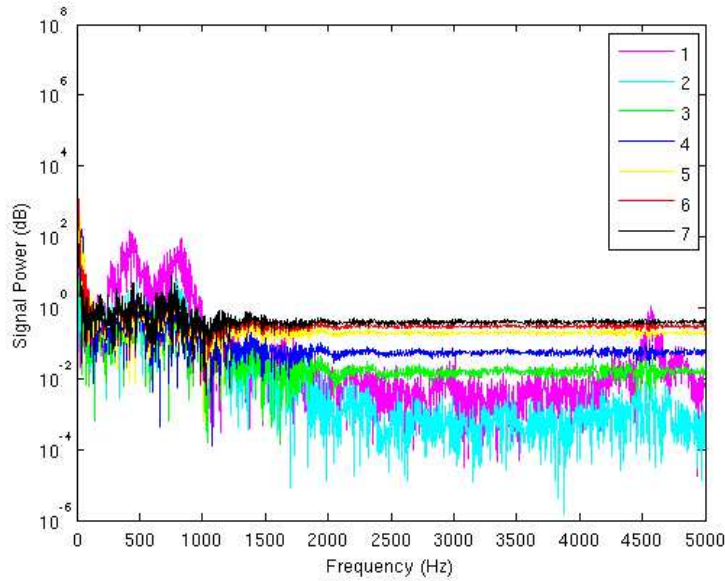
42

Figure 4.14:   PSD for each of the 7 pressure taps for the bulk-shed dimple

of oil flow lines, vortex cores, and vorticity isosurfaces, the dimple re-stabilizes with a pinned vortex near the aft of the dimple. This overview provides a general description of flow dynamics in this category, but it must be noted that the flow does not always behave exactly this way.

4.3.1 Stable Period.   Flow during the stable period strongly resembles the flow in dimples categorized as quasi-steady. Throughout most of this period, there are one or two pinned vortex cores as revealed by surface flow sinks. During the period of relative stability, vorticity isosurfaces and vortex cores suggest that fewer, or at least smaller, vortices appear to shed from the dimple. This seems to be corroborated by the small pressure variations recorded by the pressure taps between peaks, especially so for the taps nearest the dimple. (Larger variances in downstream pressure taps can be attributed to dissipation of pressure waves; as the pressure waves move downstream they become less well defined as they have less peak strength and longer duration. Also, the mesh becomes much coarser downstream of the dimple. This reduces the accuracy of pressure readings.) The flow during the stable periods shows general similarity between occurrences. Throughout each stable period there
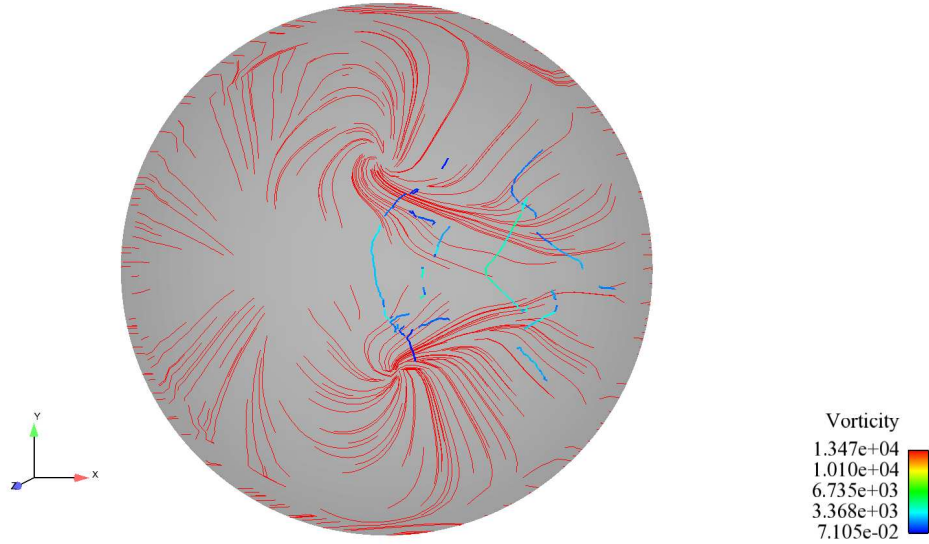
43

Figure 4.15:   Typical flow behavior during stable period of bulk shed dimple flow

is at least one, often two, sinks as revealed by surface flow visualization. Each stable period also shows highly asymmetric behavior. While the sinks are usually about the same spanwise distance away from the middle of the dimple, they were at different streamwise locations. The sinks moved in the streamwise direction at different rates.

Figure 4.16 shows the the vector plot for stable flow in the bulk shed category; it is very similar to the velocity profiles observed in the quasi-steady category (Figure 4.9). Evident in the velocity profile is the wake region, similar to the quasi-steady dimples. This dimple also shows a strong shear layer with low magnitude reversed flow filling most of the dimple below the shear layer and upstream of the wake region.

Vorticity isosurfaces reveal other similarities between the steady period and the quasi-steady dimples. During the steady periods there were a series of medium strength spanwise vorticies in the front half of the dimple. Figure 4.17 below displays typical vorticity isosurface behavior during a steady period. These medium strength vortices form a heart from about 25% of the streamwise dimple length to about the midpoint of the dimple. High strength vortices regularly shed from just behind this heart. The shedding of these vortices accounts for the 500Hz spike in the PSD plot (Figure 4.14). The shed vortices come from about the same location throughout
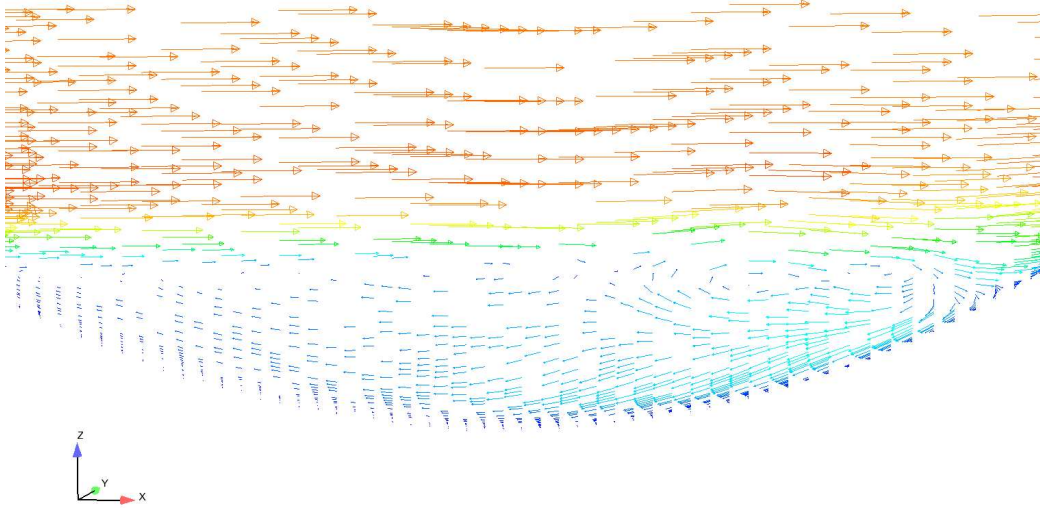
44

Figure 4.16:   Velocity profile typical of stable period of bulk shedding category

the stable period, near the center of the dimple, just behind the heart. The heart and shedding behavior is similar to the quasi-steady Re_D 20500 Re_x 77000 0.15 h/D dimple. It must be noted, though, that the heart shape is not perfectly consistent. It may grow in size and stretch to either side, but the general form, that of a cluster of streamwise vortices just in front of the center of the dimple, is a consistent feature of the stable period. In this respect, it does differ from the hearts observed in the quasi-steady dimples. The quasi-steady dimple hearts were much more consistent in location. The changing shape of the heart in the bulk-shed case does not necessarily tie into instability; the heart displayed stability while being pulled to one side.

Figure 4.18 reveals that, as with the quasi-steady dimples, the highest vorticity seems to be concentrated in the shear layer along the mouth of the dimple. Some medium and high strength vorticity isosurfaces are present in the wake region in the rear of the dimple. This, along with the velocity profile plot (Figure 4.16), suggest that, as with the quasi-steady dimples, the bulk of dimple activity takes place within the wake region and in the shear layer.
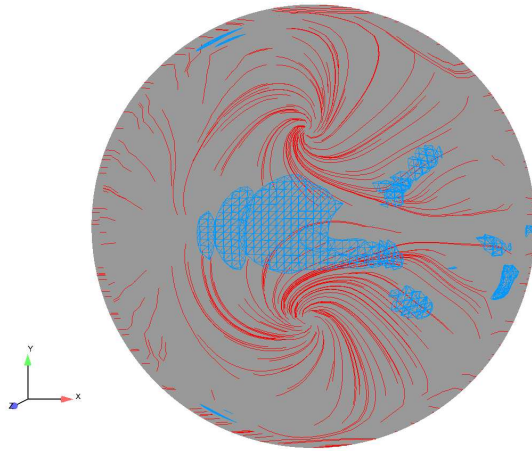
45

Figure 4.17:   Vorticity isosurface formation during typical stable period
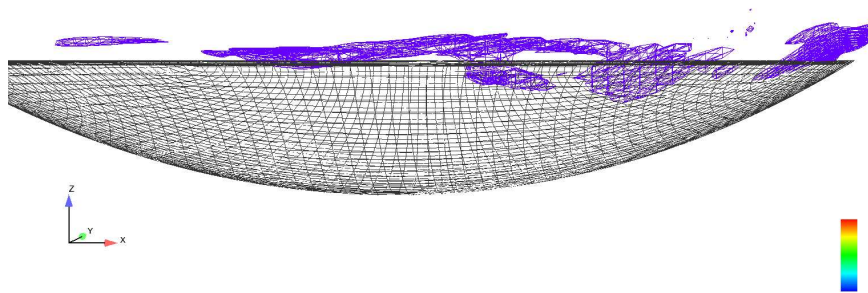

Figure 4.18:   Profile view of medium strength vorticity isosurfaces typical of stable period
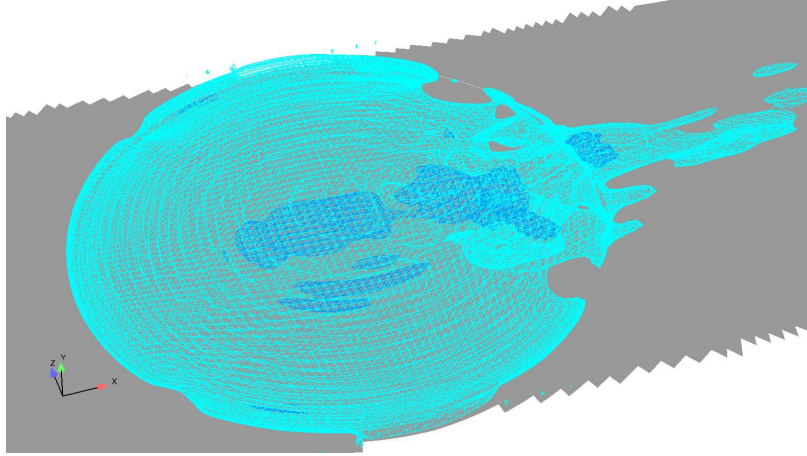
Figure 4.19:   View of low (light blue) and medium (blue) stength vorticity isosurfaces in and downstream of the dimple

Beyond the dimple, vortex strength reduced quickly. The medium and high strength vorticies do not exist far beyond the dimple. However, as shown in Figure 4.19, distinct streamwise vortex structures existed downstream of the dimple at a low strength.

The pinned vortices revealed by the surface flow sinks (Figure 4.20) typically start near the aft of the dimple and move forward during the stable cycle. However, this period has a large degree of unsteadiness in and of itself; stable is accurate only in comparison to the bulk shedding period. Sinks coalesced not only on the back of the dimple, but nearer the middle as well. The sinks appear to move over a greater area during the stable periods of this case than those in the quasi-steady category. These organized flow features, however, are not stable. Occasionally the heart will deform and the pinned vortices will dissolve as several medium and strong vortices are shed as the dimple enters an unstable period.

4.3.2   Unsteady Period.   The bulk shedding periods do not show much exact duplication between occurrences. However, a few trends carry through. Figure 4.21 shows one such trend, the large number of vortex cores in the dimple during an unsteady period. This large number of independent cores, rather than a smaller
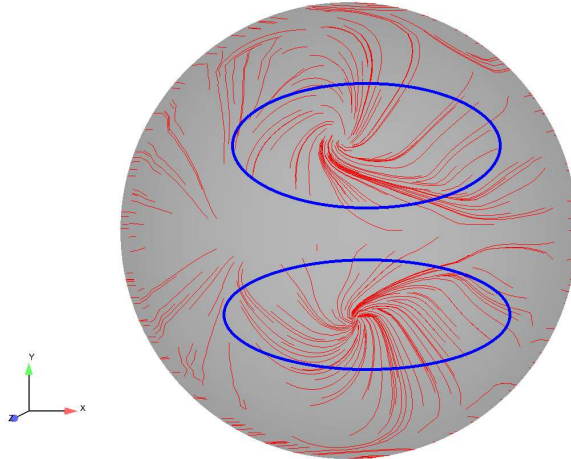
47

Figure 4.20: Surface flow sinks showing pinned vortex locations; usual regions in which these sinks move are cricled

number of larger cores seen during the steady period (Figure 4.15), suggests the breakup of vortices within the dimple.

Also during the unsteady cases, there is a distinct lack of persistant surface flow sinks. As the unsteady period begins, both sinks break up. Each side attempts to return to stability independently as the pinned sources attempt to re-develop, as shown by surface flows in Figure 4.22. It appears that the dimple begins to return to stable flow when a vortex core contacts the surface of the dimple far enough back and near the edge of the dimple to become pinned and, from there, develop.

During each unsteady occurrence, there are large pressure waves shed from the dimple that propagate downstream, as revealed by the pressure plots (Figure 4.13). Examination of vorticity isosurfaces reveal a possible explanation. As unstable periods begin, the spanwise vortices making up the heart of the dimple begin to break up as they are pulled to one side of the dimple and acquire a streamwise orientation (Figure 4.23). As this occurs, more strong vortices are shed from the dimple as the pressure taps detect larger pressure waves. Figure 4.23 shows the heart beginning to pull to one side and break up. The breakup of the heart does not happen the same way with each onset of unsteadiness. While it usually happens as a surface sink
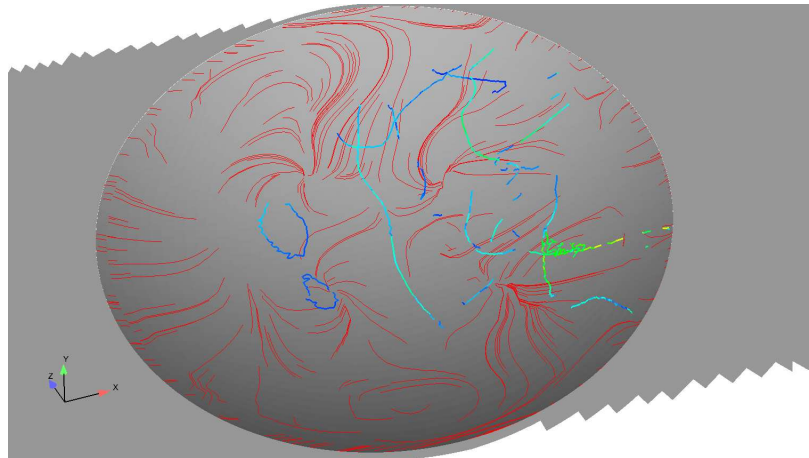
Figure 4.21:   Flow during unstable period of bulk shedding category where the colored lines are vortex cores
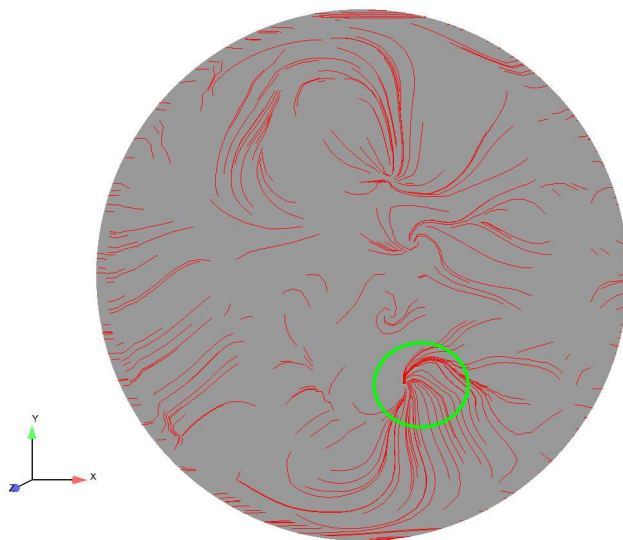

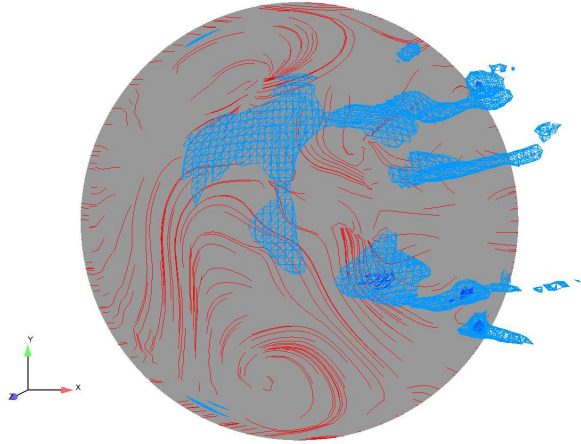Figure 4.22:   Surface flow sink attempting to reform circled

49

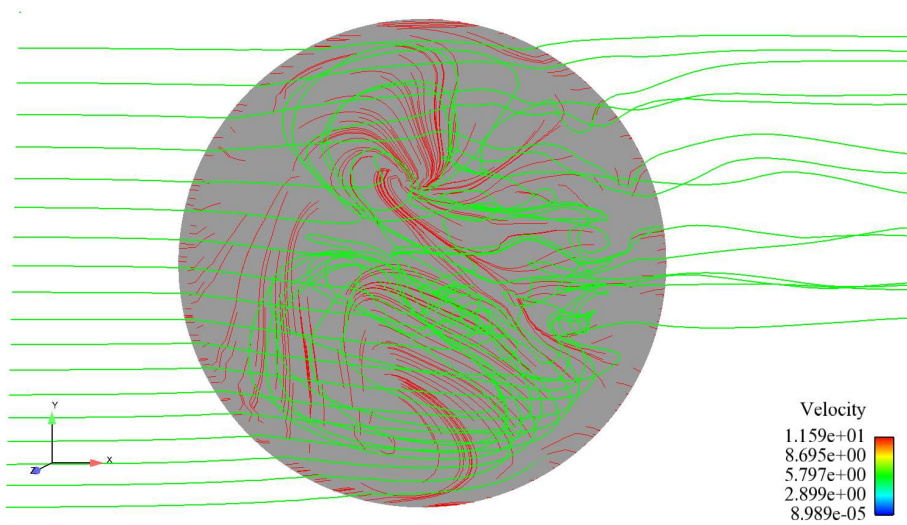Figure 4.23:   Vorticity isosurface behavior in unstable period

Figure 4.24:   Streamline behavior in unsteady period

moves forward and breaks up, sinks were observed to break up without destabilizing the entire dimple.

Another common feature of the onset of unstable periods is the shift of flow towards one side of the dimple. Particle traces originating at a rake upstream of the dimple just above the bottom of the domain reveal this motion (Figure 4.24). However, as with the breakup of surface sinks, the shift of flow to one side or another is not always followed by the bulk shedding.

It seems that the onset of the unstable periods is the result of a combination of factors. The side to side motion, pulling of the heart to one side, and breakup of surface sinks all come into play to cause a bulk shed. The return to stability shows a more consistent process.

As the heart loses structure, the strong vortices are shed less. This leads to the sudden decrease in pressures detected by the pressure taps. The vortex activity in the dimple begins to settle down; however, the heart does not immediately return. It takes some time for the heart to begin to reform, but once it has begun, it reforms quickly. First, surface sinks begin to appear. As one is able to stably coalesce and begin to move forward, the heart begins to reform. Figure 4.25 shows the sudden reforming of the heart after an unsteady period. To get an idea of how fast the heart reforms, if the typical duration of the unsteady period is used as a time scale (it usually lasts about 0.05 s) then the heart reforms over about 1% of the time scale. The reformation of the heart signals the beginning of a new stable period. Apparent in figure 4.25 are stable surface sinks, which accompany the reformation of the heart.

4.3.3 Comparison with Vincent.   The behavior for this case seems much like that for Vincent's geometry at a dimple depth to diameter ratio of 0.1 for the same case. Both showed the same steady flow, with movement of pinned vortices in the dimple similar to the quasi-steady dimples. Vincent's data suggested a large wake region and occasional bulk shedding for this case. The overall flow patterns suggest that these dimples have flow that is qualitatively very similar.

4.4 Chaotic Category

This category (the Re_D 20500 Re_x 5000 0.15 h/D dimple) is perhaps the most unique. The pressure tap data (Figure 4.26) suggests highly active flow throughout the domain in and downstream of the dimple. Strikingly, the pressure tap data is almost the exact same for each of the pressure taps. The pressure taps follow the same pattern, with spikes and valleys in the same places. The values are stacked
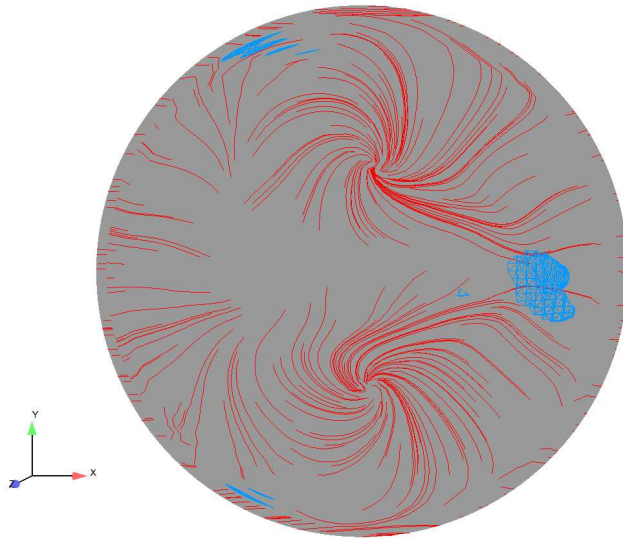
(a)
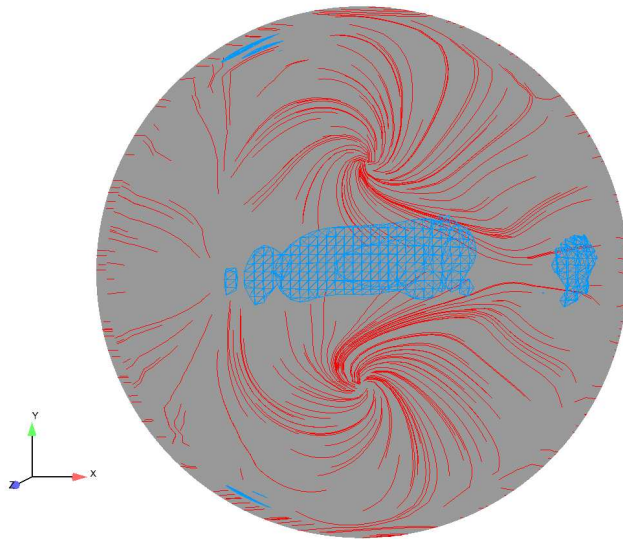
(b)

Figure 4.25:   (a) Vorticity isosurfaces at end of unstable period (b) Vorticity isosurfaces about 5ms after (a)
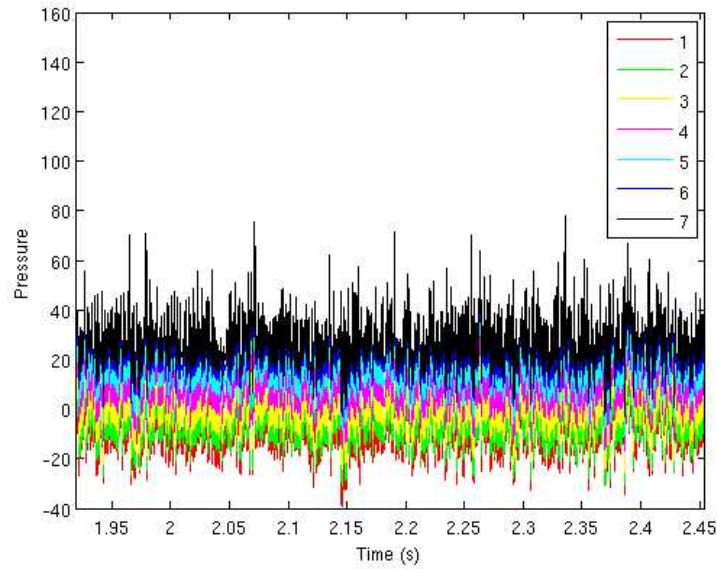
Figure 4.26: Pressure tap data for each of the 7 pressure taps of the bulk shed dimple

right on top of each other. The spikes appear at a fairly high frequency throughout the domain, but the several large spikes in pressure stand out. As with the 0.15 quasi-steady dimple, this pressure tap data suggests a continuous shedding of pressure waves from the dimple.

The PSD plot (Figure 4.27) for this case also differentiates it from the other cases. It shows no firm peak, even at the beginning of the time domain. The PSD plot makes it appear as though this case is largely noise; however, the magnitudes and pattern of the pressure tap plot suggest that there may be more going on than random noise motion. In any case, the large amount of activity at the dimple and throughout the domain suggest the dimple is having some effect on the downstream flow.

The chaotic category showed behavior different from all other categories. Principally, it lacked any of the organized structure seen in the other categories. Figure 4.28 shows a typical state of this case, with surface flow lines and vorticty isosurfaces. Animations of this case revealed a high degree of activity, although little overall pattern
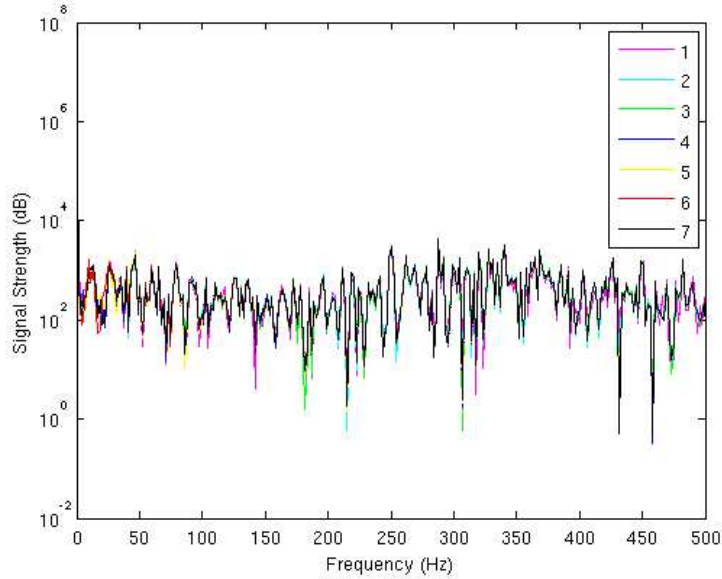
53

Figure 4.27:   PSD for each of the 7 pressure taps for the choatic dimple

or structure could be observed. The flow for this category appeared most similar to the unsteady period flow of the bulk shed category. This is of little help in characterizing the flow; the trends noticed with the unsteady flow of the bulk shed category were formed in association with departure from or return to stable flow.

Surface sinks denoting pinned vortices were a prominent feature of the quasi-steady and bulk shed categories. However, such sinks were not observed to form and stabilize in this category, as shown in Figure 4.29. Consistent vortex structure was absent as well, as revealed by the size and number of independent vortex cores. Figure 4.28 shows the disorganized surface flow and vortex cores, very similar to the unsteady period of the bulk-shed dimple.

Small regions of medium and high vorticity moved through the wake region and shed throughout the observed time domain. Low and medium strength regions of vorticity on the bow and on the sides of the dimple show more stability (Figure 4.30). Examination of these isosurfaces suggest that the flow is curling over the lip of the dimple as it crosses in, and then quickly transition to turbulent motion. No heart is observed in this case as was observed in the quasi-steady and bulk shed categories.
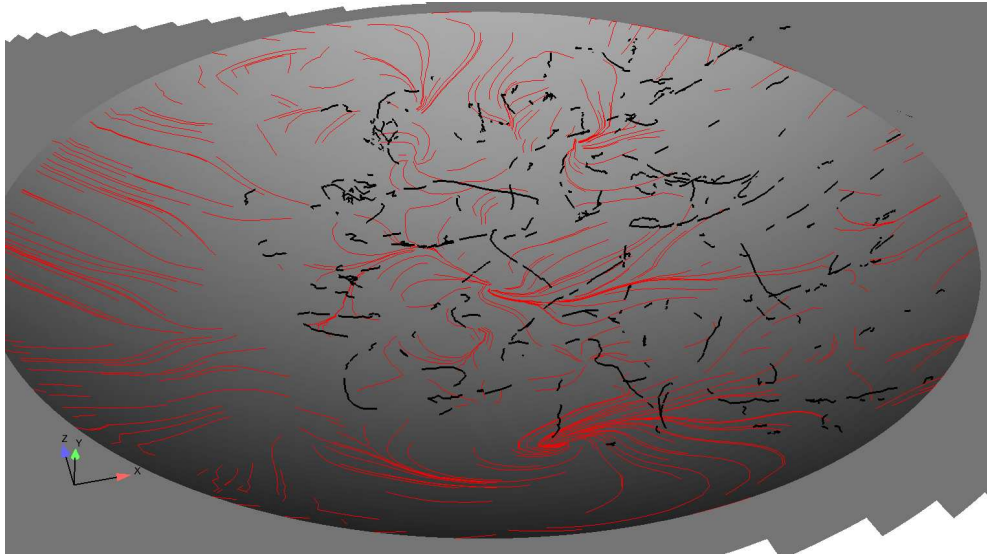
Figure 4.28:   Overview of flow in the chaotic dimple, black lines denote vortex cores
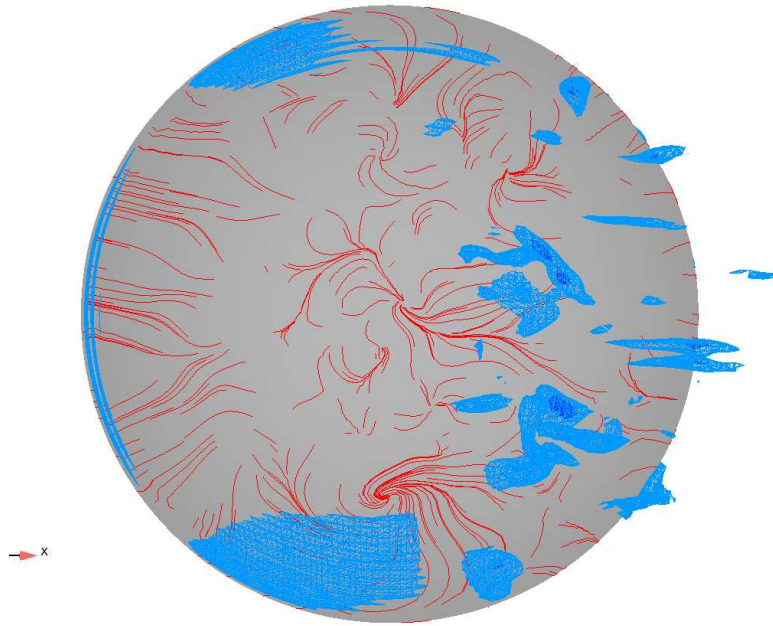

Figure 4.29:   Surface flow and vorticity isosurfaces in the chaotic dimple
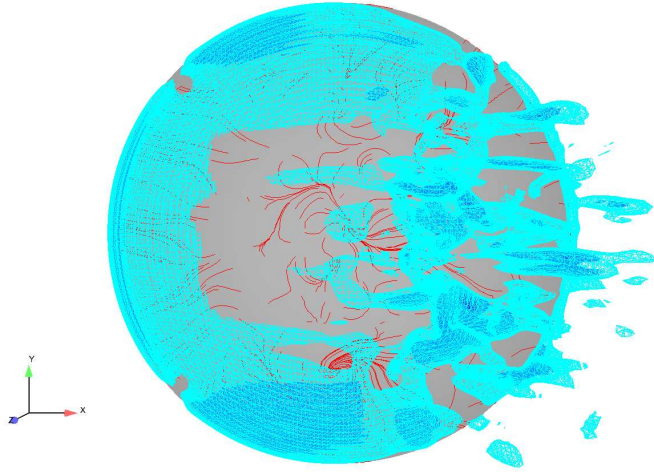
55

Figure 4.30:   Vorticity isosurfaces of low (light blue), medium (blue) and high (dark blue) strength in the chaotic dimple

Interestingly, the region where the heart resides in the other categories is in this case a region of very low vorticity (below the low-vorticity threshold).

The existence of pinned vortices and a vorticity heart were important characteristics of flow for the quasi-steady category and the stable period of the bulk shed category. Given their absence in this category, the highly unsteady nature of the flow through this dimple is of little surprise. This category and the unsteady period of the bulk shed category suggests that stable pinned vortices are an important feature to heart formation and stable dimple flow.

Figure 4.31 below showing the velocity profile along the chordwise center line of the dimple reveals other differences between this case and the others. The wake region is much larger here than in the other cases. The spanwise vortices in the aft half of the dimple reach almost to the spanwise centerline of the dimple. This larger wake region contributes to the behavior of the flow within the dimple. As observed in the quasi-steady and bulk flow cases, the pinned vortices as identified by the surface flow sinks are an important part of dimple flow behavior. The presence of a strong, large wake region and strong spanwise vorticties that fill more of the dimple than in other categories may be preventing these structures from forming.
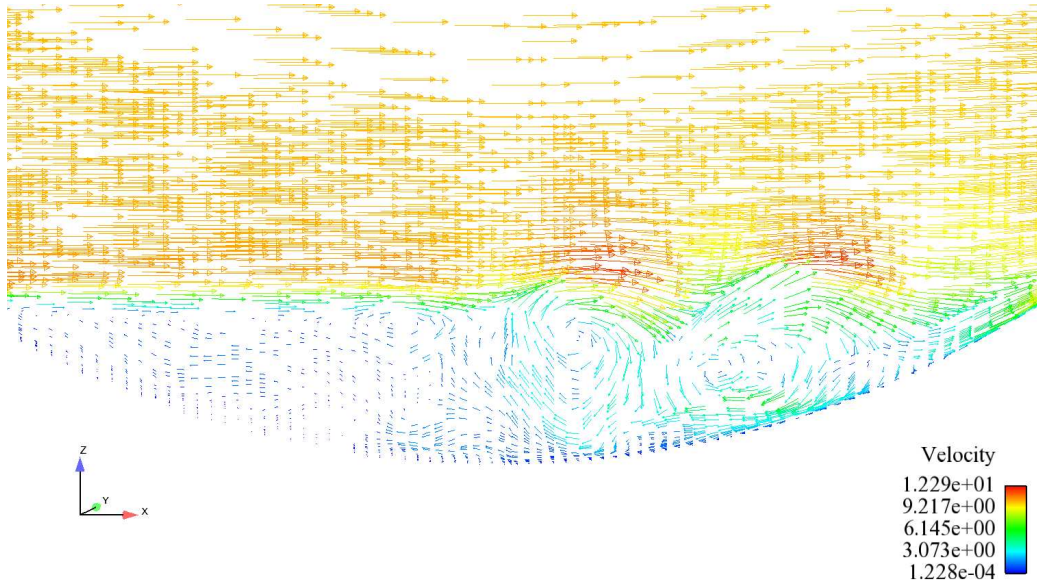
56

Figure 4.31:   Sample velocity profile of chaotic flow category

The question remains as to why this case contains such irregular flow and such a large wake region. The streamwise centerline velocity (Figure 4.31) profile may offer some insight. In each dimple case so far, large amounts of vorticity have resulted from the gradients across the shear layer over the dimple mouth. This vortical motion can mix air from above the shear layer into the dimple. This case has the smallest boundary layer, and so higher speed air is mixed into the dimple, causing larger velocity magnitudes to exist within the dimple.

This dimple, like the other two 0.15 h/D depth to diameter ratio dimples, behaves much like Vincent's 0.10 h/D dimple at the same case. Both this dimple and Vincent's showed high unsteadiness and continually variable flow with little discernable pattern.

4.5   Downstream Effects

Examination of planes normal to the chordwise direction just downstream of the dimple can help show how the dimple is influencing downstream flow. Figure 4.32 compares a profile just downstream of the Re_D 9500 Re_x 21000 0.15 h/D dimple (typical of the stable period bulk shed dimple and of the quasi-steady dimples) to

the chaotic Re_D 20500 Re_x 5000 0.15 h/D dimple. The white arrows depict velocity vectors; the non-chordwise components have been tripled to show the swirling motion of the downstream flow. This swirling flow matches the changes in the chordwise velocity contour plots. The contour plots suggest in both cases a mixing of downstream flow. High speed flow is drawn down nearer the surface in some areas, and in others low speed flow is drawn up into the freestream. The chaotic profile shows far more disorganization than the other profile.

Even the flow immediatly downstream of the dimple (where Figure 4.32 was taken) is likely very turbulent. The laminar flow solver used in this investigation will not able to resolve turbulent flow. The region just downstream of the the dimple has a much higher grid density than the far downstream region, but the density is still too low for turbulent flow. Hence, Figure 4.32 is useful for providing a possible overview of downstream flow, but is prone to error. Any analysis or conclusions made about flow downstream dimple for this grid and laminar solver are somewhat speculative.

4.6   Effect of Depth on Dimple Flow

The difference in flow between the 0.05 h/D dimples and the 0.10 h/D and 0.15 h/D dimples for the same conditions suggest that there may be a threshold value of depth to diameter ratio necessary to trip the flow from a nearly steady fixed separation bubble to more dynamic flow involving vortex movement. Vincent [14] had several dimples that would fit the steady category. All of these dimples were at his lowest tested dimple diameter, and each had a depth to diameter ratio of 0.10. Vincent's data suggests that the threshold for tripping to more unsteady behavior is not dependent upon depth to diameter ratio alone, but that depth by itself may play a role. The data of this investigation shows that depth alone will not determine if flow through a dimple acts as a nearly steady separation bubble.

The behavior observed in the 0.15 h/D dimples matched the behavior described by Vincent for each case. This consistent similarity suggests that increasing the dimple depth to diameter ratio from 0.10 to 0.15 does not significantly alter flow
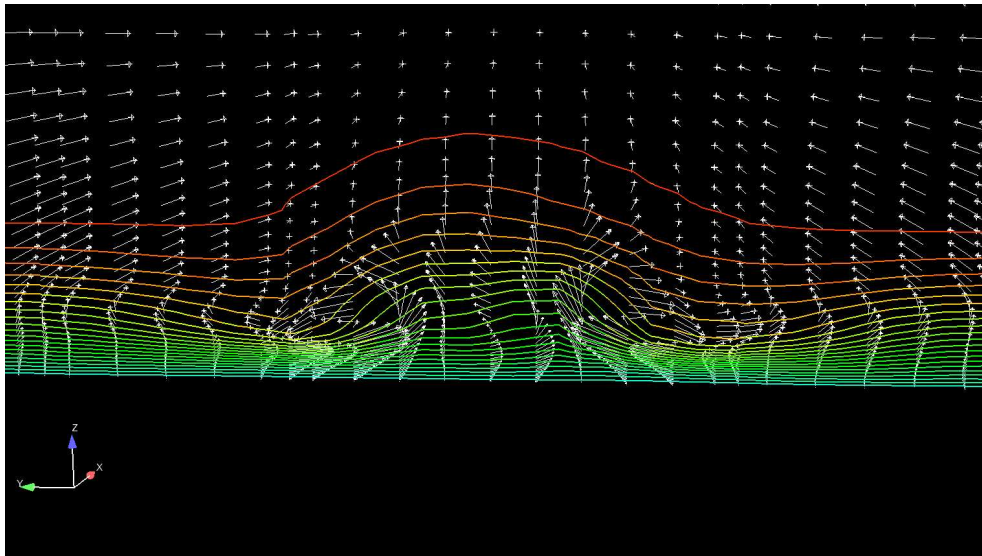
(a)
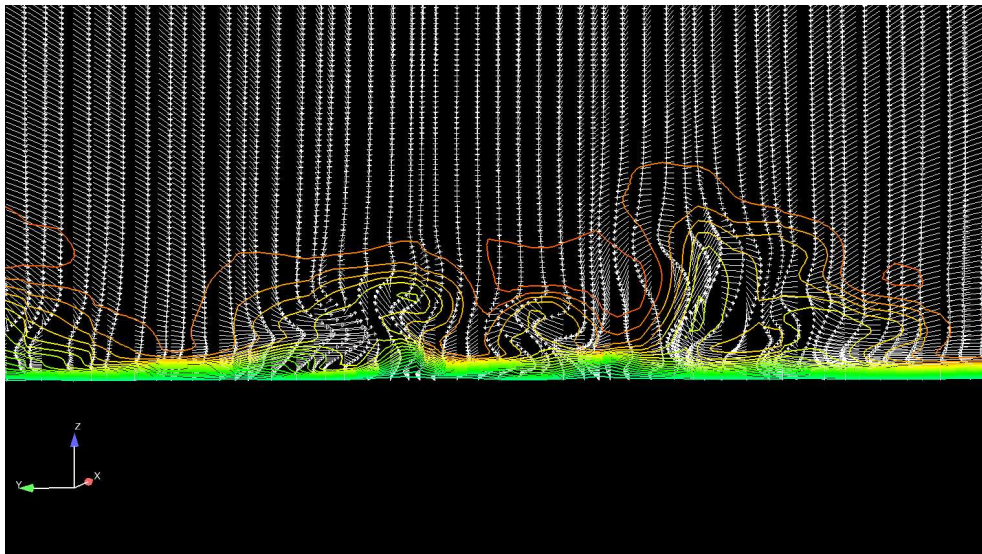
(b)

Figure 4.32:   Velocity vectors with non-chordwise components tripled and chordwise velocity contours for (a) Re$_D$ 9500 Re$_x$ 21000 0.15 h/d dimple and (b) Re$_D$ 20500 Re$_x$ 5000 0.15 h/D dimple

dynamics. However, for a dimple depth to diameter ratio of 0.25, the dimple flow changed noticeably. The flow for the 0.25 h/D dimple did not show the bulk shedding observed in the 0.15 h/D dimple for the same case. The 0.25 h/D dimple flow was much more like that of the quasi steady 0.15 h/D dimple for the Re_D 20500 Re_x 77000 case, yet it showed much less downstream effect. The pressure taps for the 0.25 h/D dimple resemble most closely the dimples for the 0.05 h/D dimples. The swallowing phenomenon offered in section 4.2.1 to explain this behavior has the consequence that increases in dimple depth to diameter ratio can begin to dilute the downstream effects of the dimple.

4.7   Characteristics of Dimple Flow

The observations made suggest that flow through a dimple is a highly unsteady phenomenon dependent upon many factors. However, this investigation revealed several qualities that may aide in studying and characterizing dimple flow in the future.

Vincent [14] suggested that dimples that can maintain stability while shedding vortices at high frequency are most beneficial to preventing downstream separation. The dimples which showed some of this behavior, at least for some time, all contained a heart of streamwise vortices. These vortices appeared to originate from flow coming over the leading edge of the dimple. The vortices shed by the dimple appeared to be shed from the heart.

The existence, stability, and motion of the pinned vortices are strong indicators of the flow within the dimple. Flow coming in from the sides of the dimples becomes entrained in these vortices. The pinned vortices appeared to encourage vortex shedding from the dimple heart. Also, the stability of the flow is indicated, to some degree, by the behavior of the pinned vortices. The flow in the bulk shed category would not go unstable unless one of the surface sinks broke up.

Attempts to quantify dimple geometry effects on dimple flow proved elusive. A variety of parameters (diameter, depth, chordwise location, boundary layer thickness,

volume), ratios (depth to diameter, depth to boundary layer thickness, diameter to boundary layer thickness, etc.) and combinations thereof were examined to try and determine trends relating to flow category. However, between the data of this and Vincent's investigation, no parameter or combination was found that could give a strong, meaningful pattern to flow category.

In spite of the difficulty in divining quantitative parameters of dimple flow, some observations regarding qualitative flow characteristics and trends may be made. The flow similarity between the current shallow (0.05 h/D) and Vincent's small diameter dimples suggests that both diameter and depth to diameter ratio influence dimple flow. The difference between the Re_D 20500 Re_x 5000 and Re_D 20500 Re_x 77000 cases revealed by the 0.10 h/D and 0.15 h/D dimples show that boundary layer thickness can have a strong influence on dimple flow.

The following overview of dimple flow structure is offered. If a dimple is too shallow (low depth to dimaeter ratio) or of too small total depth, the dimple will generate a fixed separation bubble rather than the more desirable dynamic vortex behavior. As the dimple becomes large enough to generate shedding vortices, boundary layer thickness, especially in relation to dimple diameter, becomes more important. A thin boundary layer will result in highly disorganized dimple flow. As the boundary layer grows thicker, the dimple flow will stabilize. The disorganized flow becomes constrained to certain periods between periods of more stable flow, and eventually vanishes as the boundary layer grows thicker. Further increases of dimple depth beyond that necessary to generate vortex shedding seem merely to entrain more flow in the dimple while reducing downstream effect. As dimple depth to diameter ratio increases, more flow is moved from the dynamic environment of the shear layer to the more benign environment in the bottom of the dimple.

V. Conclusions

The dimple depth to diameter ratio was found to have a noticeable effect on flow through the dimple. In all investigated flow regimes, the flow through a very shallow (depth to diameter ratio of 0.05) dimple was found to be nearly steady, even if the flow for the same case with depth to diameter ratio of 0.10 was highly chaotic. Dimples of a depth to diameter ratio of 0.15 were found to behave very similarly to the same case with a depth to diameter ratio of 0.10 as investigated by Vincent [14]. A dimple depth to diameter ratio of 0.25 seemed to swallow much of the flow mixing and reduce the downstream effect of the dimple.

Several characteristics shared among many of the non-shallow dimples were identified. In the three that displayed non-chaotic motion (0.15 h/D Re_D 9500 Re_x 21000, 0.25 h/D Re_D 9500 Re_x 21000, and 0.15 h/D Re_D 20500 Re_x 77000), a vortex heart existed in the middle of the dimple along the shear layer. From this heart are shed vortices at a high frequency. Also in the three non-chaotic cases, the behavior of the pinned vortices seemed to have a strong influence on the dimple flow; stable, regular vortex motion would lead to a stable overall dimple. However, the breakup of the pinned vortices contributes to de-stabilization and can move the entire dimple to bulk flow. This results in a short increase in shed vorticity followed by a lapse in vortex shedding.

High speed, continuous vortex shedding is desirable for greater flow mixing (as established by Ligrani [7]). This suggests that the shallowest dimple possible (lowest depth to diameter ratio) be used that will be sufficient for activating non-steady flow. If the dimple is too shallow, the dimple will not affect the flow sufficiently. A dimple beyond the depth necessary to develop pinned and shedding vortices will only serve to entrain more flow in the slow, bottom part of the dimple. The dimples in Lake's [6] wind tunnel investigation all showed behavior similar to the steady category of dimples. Further improvments in flow separation performance may be obtained by increasing the depth of these dimples.

5.1 Suggestions for further research

While this investigation was able to identify effects of changing dimple depth to diameter ratio on dimple flow, it did not completely separate depth from diameter effects. Examination of more depth to diameter ratios in the quasi steady, bulk shed, and chaotic categories may establish a definite difference (i.e., which has a greater effect) between depth and diameter in these flow categories.

The observations made in this investigation suggest several possible avenues for further research. Only one 0.25 h/D dimple was studied. It may be beneficial to examine 0.25 or greater depth to diameter ratio dimples for other cases to determine whether the trend observed in the cases studied is consistent with other geometries. It may also be informative to look at dimple depth to diameter ratios between 0.15 and 0.25 to see if there is a definite trend towards the dimple swallowing flow and reducing downstream effects, as suggested by this investigation. Also, confirmation of the transition from chaotic to quasi steady flow described could be verified by examination of many depth to diameter ratios with a constant chordwise location with particular attention to duration of unsteady periods.

The observations drawn and conclusions made about flow downstream of the dimple, and hence the effect of the dimple on the flow, are somewhat speculative. The flow downstream of the dimple has been observed to have significant turbulence levels [6], and laminar flow models were used for this and previous numerical investigations into dimple flow [10], [2], [14]. A Large eddy simulation may be able to model the separation behavior necessary for dimple study while confirming or correcting earlier conclusions made about downstream flow effects.

An extensive study on optimum dimple shape and effect of dimple shape on flow has not been made. Rouser [10] examined only two very broad shapes, an ellipse and a half ellipse. Dimples with different surface geometries (i.e. a square instead of circle mouth) may provide different flow characteristics. Changes may also arise

from using different shapes of the bottom of the dimple, such as giving the dimple a teardrop cross section rather than making it from a section of a sphere.

Further efforts to characterize dimple flow, either in terms of overall structure or in more specific terms such as vortex shedding frequency, quantitatively may see more success than the efforts of this investigation. Such quantifications, if they could be made, would assist greatly in optimizing dimples for use in low pressure turbine blades.

VI. Additonal Comparison Figures
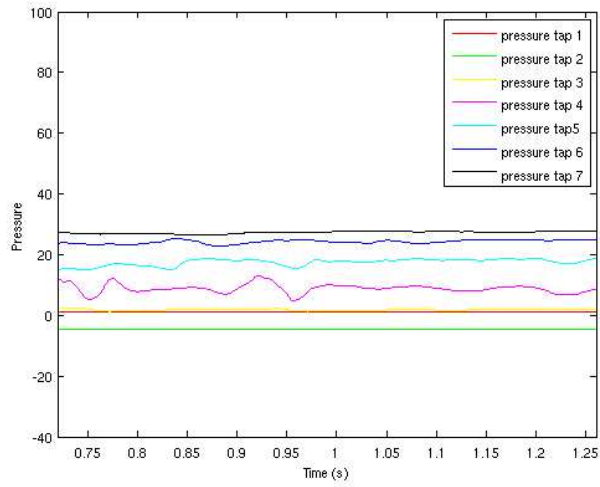
Figure F.1:   Pressure tap for Re$_D$ 20500 Re$_x$ 5000 0.05 h/D dimple.
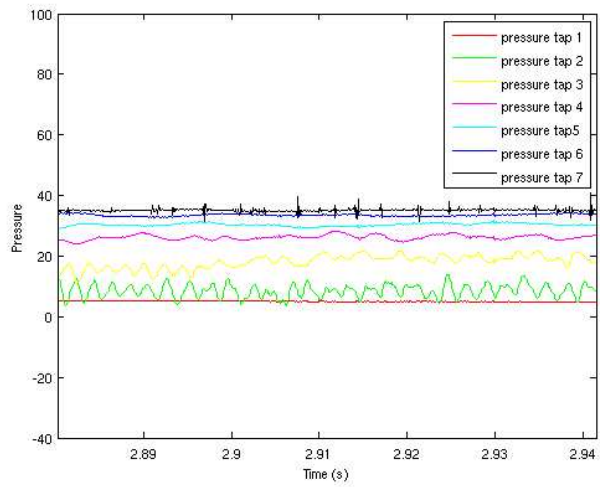
Figure F.2:   Pressure tap for Re$_D$ 20500 Re$_x$ 77000 0.05 h/D dimple.
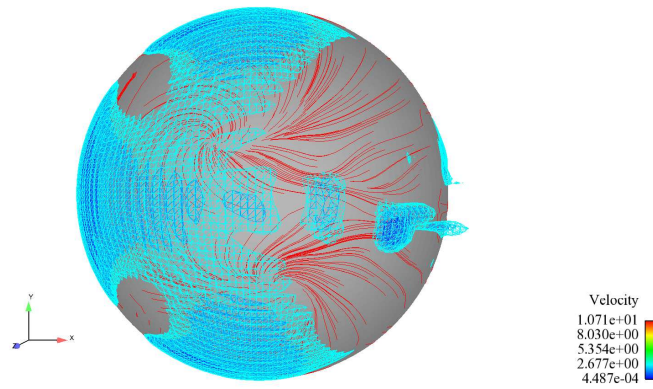
Figure F.3:   Vorticity isosurfaces for Re_D 9500 Re_x 21000 0.25 h/D Dimple
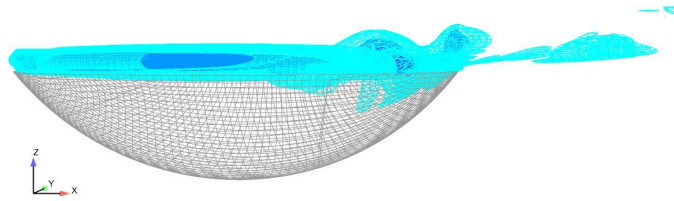

Figure F.4:   Vorticity isosurface profile for Re_D 9500 Re_x 21000 0.25 h/D Dimple
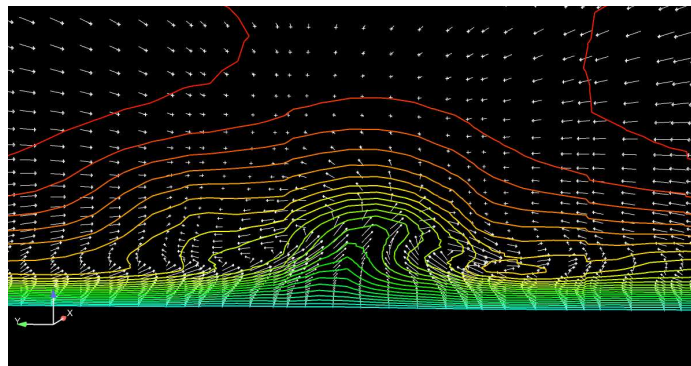

Figure F.5:   Downstream velocity profile for Re_D 9500 Re_x 21000 0.25 h/D Dimple
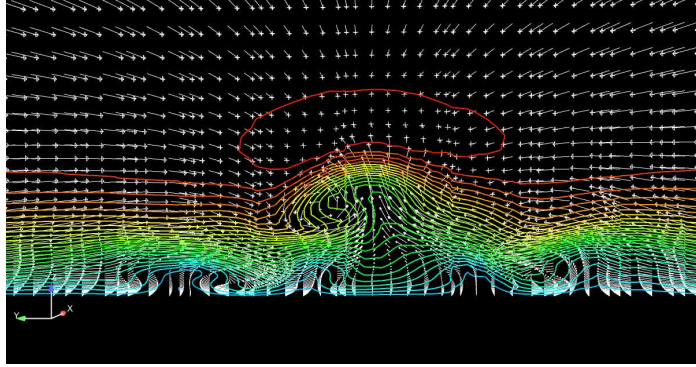
Figure F.6: Downstream velocity profile for Re_D 20500 Re_x 77000 0.15 h/D Dimple
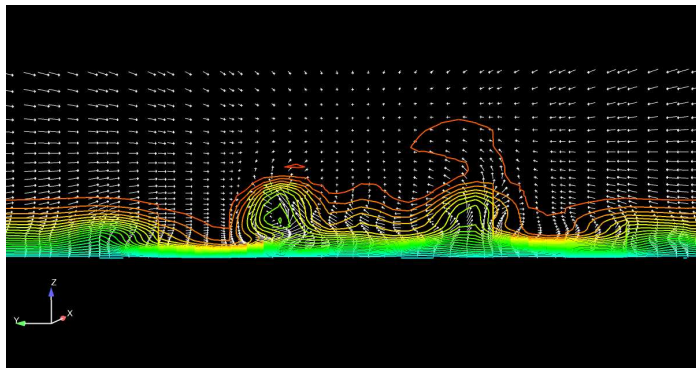

Figure F.7: Downstream velocity profile for Re_D 9500 Re_x 21000 0.15 h/D Dimple during unstable period

Bibliography

1. *Computational Fluid Dynamics: Principles and Applications.* Elsevier, 2005.

2. Casey, J. P. *Effect of Dimple Patter non the Suppression of Bounary Layer Separation on a Low Pressure Turbine Blade.* Master's thesis, Air Force Institute of Technology, 2004.

3. Computational Engineering International, Inc., 2166 N. Salem Street, Suite 101, Apex, NC. *Ensight Users Manual for Version 8.2*, 2006.

4. Fluent, Inc., Lebanon, NH. *Fluent 6.2 User's Guide*, 2005.

5. Grace, M. S., W. G. Dewar, and D. E. Wroblewski. "Experimental Investigation of the Flow Characteristics Within a Shallow Wall Cavity for both Laminar and Turbuelnt Upstream Boundary Layer". *Experiments in Fluids*, 36, 2004.

6. Lake, J. P. *Flow Separation Prevention on a Turbine Blade in Cascade at Low Reynolds Number.* Ph.D. thesis, Air Force Institute of Technology, 1999.

7. Ligrani, P. M., J. L. Harrison, G. I. Mahmmod, and M. L. Hill. "Flow Structure Due to Dimple Depressions on a Channel Surface". *American Institute of Physics*, 13, 2001.

8. Maple, R. C., R. Osterday, and R. Vickery. "Fluent VTK Extractor".

9. Ozsoy, E., P. Rambaud, and M. L. Rieghmuller. "Vortex Characteristics in Laminar Cavity Flow at Very Low Mach Number". *Experiments in Fluids*, 38, 2005.

10. Rouser, K. P. *Use of Dimples to Suppress Boundary Layer Separation on a Low Pressure Trubine Blade.* Master's thesis, Air Force Institute of Technology, 2002.

11. Schroeder, William, Kenneth Martin, and William Lorensen. *The Design and Implementation of an Object-Oriented Toolkit for 3D Graphics and Visualization.* Technical report, GE Corporate Research and Development, 2004.

12. Sujudi, David and Robert Haimes. *Identification of Swirling Flow in 3-D Vector Fields.* Technical report, Masschusetts Institute of Technology, 1995.

13. Syred, N., A. Khalatov, A. Kozlov, A Shchukin, and R. Agachev. "Effect of Surface Curvature on Heat Transfer and Hydrodynamics Within a Single Hemispherical Dimple". *Journal of Turbomachinery*, 123, 2001.

14. Vincent, R. C. *CFD Investigation of the Flow Dynamics Inside a Spherical Surface Indentation.* Master's thesis, Air Force Institute of Technology, 2006.

1. REPORT DATE *(DD-MM-YYYY)* 14 Jun 07	2. REPORT TYPE Master's Thesis		3. DATES COVERED *(From – To)* Jun 2006 – Jun 2007

4. TITLE AND SUBTITLE CFD Investigation of Effect of Depth to Diameter Ratio on Dimple Flow	5a. CONTRACT NUMBER
	5b. GRANT NUMBER
	5c. PROGRAM ELEMENT NUMBER
6. AUTHOR(S) Etter, Robert, B. Ensign, United States Navy	5d. PROJECT NUMBER
	5e. TASK NUMBER
	5f. WORK UNIT NUMBER

7. PERFORMING ORGANIZATION NAMES(S) AND ADDRESS(S) Air Force Institute of Technology Graduate School of Engineering and Management (AFIT/EN) 2950 Hobson Way WPAFB OH 45433-7765	8. PERFORMING ORGANIZATION REPORT NUMBER **AFIT/GAE/ENY/07-J07**
9. SPONSORING/MONITORING AGENCY NAME(S) AND ADDRESS(ES) Unsponsored	10. SPONSOR/MONITOR'S ACRONYM(S)
	11. SPONSOR/MONITOR'S REPORT NUMBER(S)

12. DISTRIBUTION/AVAILABILITY STATEMENT APPROVED FOR PUBLIC RELEASE; DISTRIBUTION UNLIMITED.

13. SUPPLEMENTARY NOTES

14. ABSTRACT

This study aimed to further the understanding of laminar flow through a dimple with the goal of mitigating flow separation. Dimples of various depth to diameter ratios (0.05, 0.15) were examined for three different dimple diameters and chordwise locations, corresponding to diameter based (Re_D) and chordwise location based (Re_x) Reynolds number combinations of Re_D 20500 \Rex 5000, Re_D 20500 Re_x 77000, and Re_D 9000 Re_x 21000. For the last combination, a dimple of depth to diameter ratio of 0.25 was also examined. The dimples were placed in a flat plate located in a diverging channel causing an adverse pressure gradient encouraging flow separation near the dimple location. The flow was modeled in the commercial CFD solver Fluent. Results indicate that dimple depth to diameter ratio has a significant effect on the structure of dimple flow. The shallowest dimples showed little change to the overall flow in the channel. Deeper dimples contained dynamic vortical flow structures with behavior varying between each dimple studied. This dynamic vortex activity was observed to be linked with variances in downstream flow. The 0.15 depth to diameter ratio dimples showed behavior very similar to 0.10 ratio dimples investigated elsewhere. The 0.25 dimple show flow different in nature than 0.15 dimples for the same Re_D and Re_x; the differences were not as stark as those between 0.05 and 0.15 dimples. In light of this and other studies, dimple flow behavior is found to depend on a combination of parameters that eludes direct quantitative parameterization. However, the conclusion is drawn that the most effective dimple will be just deep enough to develop dynamic vortical activity and vortex shedding.

15. SUBJECT TERMS
Flow Separation Prevention, Laminar Flow, Dimple, Depth Effects, Depth to Diameter Ratio, Unsteady Flow

16. SECURITY CLASSIFICATION OF:			17. LIMITATION OF ABSTRACT	18. NUMBER OF PAGES	19a. NAME OF RESPONSIBLE PERSON LtCol Raymond Maple (AFIT/ENY)
REPORT **U**	ABSTRACT **U**	c. THIS PAGE **U**	**UU**	83	19b. TELEPHONE NUMBER *(Include area code)* (937) 255-3636, ext 4577; e-mail: raymond.maple@afit.edu